THE JOURNAL OF BIOLOGICAL CHEMISTRY Vol. 280, No. ??, Issue of ???? ??, pp. 1–xxx, 2005

Printed in U.S.A.

Sertoli-Germ Cell Anchoring Junction Dynamics in the Testis Are Regulated by an Interplay of Lipid and Protein Kinases*

Received for publication, January 28, 2005, and in revised form, April 22, 2005
Published, JBC Papers in Press, May 3, 2005, DOI 10.1074/jbc.M501049200

Michelle K. Y. Siu‡§, Ching-hang Wong‡, Will M. Lee¶, and C. Yan Cheng‡‖

From the ‡Center for Biomedical Research, Population Council, New York, New York 10021 and the ¶Department of Zoology, University of Hong Kong, Hong Kong, China

AQ: A

When Sertoli and germ cells were co-cultured *in vitro* in serum-free chemically defined medium, functional anchoring junctions such as cell-cell intermediate filament-based desmosome-like junctions and cell-cell actin-based adherens junctions (*e.g.* ectoplasmic specialization (ES)) were formed within 1–2 days. This event was marked by induction of several protein kinases such as phosphatidylinositol 3-kinase (PI3K), phosphorylated protein kinase B (PKB; also known as Akt), p21-activated kinase-2 (PAK-2), and their downstream effector (ERK) as well as an increase in PKB intrinsic activity. PI3K, phospho (p)-PKB, and PAK were co-localized to the site of apical ES in the seminiferous epithelium of the rat testis in immunohistochemistry studies. Furthermore, PI3K also co-localized with p-PKB to the same site in the epithelium as determined by fluorescence microscopy, consistent with their localization at the ES site. These kinases were shown to associate with ES-associated protein complexes such as β1-integrin, phosphorylated focal adhesion kinase, and c-Src by co-immunoprecipitation, suggesting that the integrin·laminin protein complex at the apical ES likely utilizes these protein kinases as regulatory proteins to modulate Sertoli-germ cell adherens junction dynamics via the ERK signaling pathway. To validate this hypothesis further, an *in vivo* model using AF-2364 (1-(2,4-dichlorobenzyl)-1*H*-indazole-3-carbohydrazide) to perturb Sertoli-germ cell anchoring junction function, inducing germ cell loss from the epithelium in adult rats, was used in conjunction with specific inhibitors. Interestingly, the event of germ cell loss from the epithelium induced by AF-2364 *in vivo* was also associated with induction of PI3K, p-PKB, PAK-2, and p-ERK as well as a surge in intrinsic PAK activity when spermatids began to dislodge from the epithelium. Perhaps the most important of all, pretreatment of rats with wortmannin (a PI3K inhibitor) or anti-β1-integrin antibody via intratesticular injection indeed delayed AF-2364-induced spermatid loss from the epithelium *versus* treatment with AF-2364 or IgG alone. In summary, these results illustrate that Sertoli-germ cell anchoring junction dynamics in the rat testis are regulated, at least in part, via the β1-integrin/PI3K/PKB/ERK signaling pathway.

AQ: B

AQ: C

In the seminiferous epithelium of the rat testis, Sertoli-germ cell adhesion function is maintained by cell-cell actin-based adherens junctions (AJs)[1] and intermediate filament-based desmosome-like junctions (for reviews, see Refs. 1–3). The best studied testis-specific AJ type is ectoplasmic specialization (ES). The ES is confined between Sertoli cells (known as the basal ES) at the site of the blood-testis barrier (BTB) as well as between Sertoli cells and spermatids (known as the apical ES) in the adluminal compartment of the epithelium (for reviews, see Refs. 3 and 4). Most of the studies on cell adhesion function in the testis in the past 2 decades have focused on the apical ES because the biochemical composition of the desmosome-like junction remains largely unexplored in the testis (for reviews, see Refs. 1, 3, and 5). The apical ES is an important anchoring junction device that provides mechanical adhesion of spermatids onto the nourishing Sertoli cells to assist movement of developing spermatids across the epithelium and to ensure proper orientation of spermatids in the epithelium so that fully developed spermatids can be released to the tubule lumen during spermiation. Without this timely event of spermatid movement, spermatogenesis cannot be completed, leading to infertility. Although the morphology of the ES has been characterized for almost 3 decades, its biochemical composition and molecular architecture have not been known until recently. Furthermore, the underlying regulatory mechanism(s) that regulates ES dynamics remains largely unexplored (for reviews, see Refs. 1, 6, and 7). However, recent studies have shown that ES dynamics are regulated by focal adhesion complex-associated proteins such as β1-integrin, focal adhesion kinase (FAK), and vinculin. Of particular interest is the hypothesis that tyrosine-phosphorylated (activated) FAK is a crucial linker between β1-integrin and other ES components at the apical ES (7, 8). As such, a better understanding of the downstream signaling pathway(s) of integrin and FAK is crucial to the study of ES dynamics. This is also important to developmental biologists because it helps unfold the under-

Fn1

* This work was supported in part by NICHD Grants U01 HD045908 and U54 HD029990 (Project 3) from the National Institutes of Health (to C. Y. C.), CONRAD Program Grant CICCR CIG 01-72 (to C. Y. C.), and Hong Kong Research Grant Council Grants HKU 7194/01M and 7413/04M (to W. M. L. and C. Y. C.). The costs of publication of this article were defrayed in part by the payment of page charges. This article must therefore be hereby marked "*advertisement*" in accordance with 18 U.S.C. Section 1734 solely to indicate this fact.

§ Present address: Dept. of Pathology, Faculty of Medicine, University of Hong Kong, Hong Kong, China.

‖ To whom correspondence and reprint requests should be addressed: Center for Biomedical Research, Population Council, 1230 York Ave., New York, NY 10021. Tel.: 212-327-8738; Fax: 212-327-8733; E-mail: Y-Cheng@popcbr.rockefeller.edu.

AQ: MM

[1] The abbreviations used are: AJs, adherens junctions; ES, ectoplasmic specialization(s); BTB, blood-testis barrier; FAK, focal adhesion kinase; PI3K, phosphatidylinositol 3-kinase; SH2, Src homology 2; PPI, polyphosphoinositide; PI-4,5-P_2, phosphatidylinositol 4,5-bisphosphate; PI-3,4,5-P_3, phosphatidylinositol 3,4,5-trisphosphate; PH, pleckstrin homology; PKB, protein kinase B; PDK1, phosphoinositide-dependent kinase-1; PAK, p21-activated kinase; MEK, mitogen-activated protein kinase/extracellular signal-regulated kinase kinase; ERK, extracellular signal-regulated kinase; FA, focal adhesion; DMEM, Dulbecco's modified Eagle's medium; TJ, tight junction; EGF, epidermal growth factor; p-, phospho-; Co-IP, co-immunoprecipitation; GSK-3, glycogen synthase kinase-3; PBS, phosphate-buffered saline; MMP, matrix metalloprotease; MAPK, mitogen-activated protein kinase.

lying mechanism that regulates junction restructuring events in the seminiferous epithelium pertinent to spermatogenesis.

Autophosphorylation of FAK at Tyr^{397} can recruit a variety of cytosolic proteins to the plasma membrane (for review, see Ref. 9). For example, phosphatidylinositol 3-kinase (PI3K) p85α, the adaptor subunit of PI3K, is one of the Src homology 2 (SH2) domain-containing proteins that bind to FAK (10, 11). Upon this binding, p85α subsequently recruits the PI3K p110 catalytic subunit to the plasma membrane, where it phosphorylates polyphosphoinositides (PPIs; predominantly phosphatidylinositol 4,5-bisphosphate (PI-4,5-P_2)) at position 3 of the inositol ring, producing a second messenger, phosphatidylinositol 3,4,5-trisphosphate (PI-3,4,5-P_3) (for reviews, see Refs. 11–13). The accumulated PI-3,4,5-P_3 acts as membrane anchor that recruits and activates pleckstrin homology (PH) domain-containing proteins such as protein kinase B (PKB; a Ser/Thr kinase also known as Akt), which is a PI3K effector (for reviews, see Refs. 11 and 12). The membrane-localized PKB is then activated via phosphorylation at Thr^{308} and Ser^{473} by a second phosphoinositide-dependent Ser/Thr kinase, phosphoinositide-dependent kinase-1 (PDK1), and a yet-to-be identified "Ser^{473} kinase," respectively. In turn, the activated PKB phosphorylates its downstream effectors at the plasma membrane, in the cytosol, and in the nucleus. Depending on the specific effector that is being activated, diverse biological processes such as glucose metabolism, cell cycle progression, apoptosis, transcription regulation, and cell motility can be modulated by PKB. The turnover of PI-3,4,5-P_3 is mediated by phosphatases, which dephosphorylate the 3′-end of the lipid, leading to a reduction of the pool of lipids capable of PKB binding, thus negatively regulating the PI3K/PKB signaling pathway. PTEN (phosphatase and tensin homolog deleted on chromosome ten) is the major lipid phosphatase that antagonizes the reactions catalyzed by PI3K (16). Interestingly, there is accumulating evidence that the PI3K/PKB pathway plays an important role in the formation and stabilization of AJs, linking AJ components to the cytoskeleton in keratinocytes, intestinal epithelial cells, mammary epithelial cells, and Caco-2/15 cells (18, 19). In the testis, PI-4,5-P_2 and phosphoinositide-specific phospholipase C have been identified in the ES (20), and the PI3K/PKB signaling pathway has recently been shown to be regulated by follicle-stimulating hormone in 20-day-old Sertoli cells (21–23). However, little is known regarding the upstream and downstream mediators of the PI3K/PKB signaling pathway in the testis and its contribution to junction dynamics, especially at the apical ES.

p21-activated kinase (PAK)-1–3 (Ser/Thr protein kinases) are direct PKB effectors (for reviews, see Refs. 12, 24, and 25). The activation of PAKs by direct binding to the active Rac and Cdc42 GTPases has been well established. In addition, PAKs can be activated through a variety of GTPase-independent mechanisms, including the direct phosphorylation by other kinases such as PKB and PDK1 (24–26). Because of their complicated activation processes and the presence of multiple substrates, PAKs serve as important modulators for a wide range of cellular processes, including cytoskeletal reorganization, cell motility, apoptosis, cell cycle progression, and cell transformation (for review, see Ref. 24). One interesting feature of PAKs is their ability to phosphorylate Raf-1 in a PI3K-dependent manner, which, along with integrin, mediates the Ras signaling pathway that leads to activation of the Raf-1/MEK/ERK signaling cascade (for review, see Ref. 25). Besides PAKs, PKB is another crucial downstream mediator of the PI3K/Raf-1 cross-talk in the Ras/Raf-1/MEK/ERK signaling pathway (14, 27). In the testis, activated ERK has been localized at the apical ES at the time of spermiation, implicating its role in ES disassembly (28). However, the precise mechanism(s) for ERK-mediated ES dynamics remains largely undefined. Furthermore, PI3K, PKB, PAK, and ERK are imperative regulators of cytoskeletal dynamics, conferring cell migration at the focal adhesion (FA) site. Because cytoskeletal rearrangement is an essential process for ES restructuring (for reviews, see Refs. 1, 2, and 7), it is possible that the PI3K/PKB/PAK/ERK pathway is the major downstream signaling cascade of integrin and FAK at the apical ES (7, 8) that regulates ES restructuring. To elucidate the involvement of these kinases in ES dynamics, the expression and activation of these signal mediators during AJ restructuring and their localization in the testis were examined in both *in vitro* and *in vivo* models. These findings further support the hypothesis that FA complex-associated proteins are involved in ES dynamics and that the ES is a hybrid cell-cell and cell-matrix actin-based anchoring junction type.

EXPERIMENTAL PROCEDURES

Animals—Sprague-Dawley rats were obtained from Charles River Laboratories, Inc. (Wilmington, MA).

Primary Sertoli Cell Cultures—Sertoli cells were isolated from the testes of 20-day-old rats (29). Cells were plated at high cell density (0.5×10^6 cells/cm^2) on 12-well dishes (Corning) coated with Matrigel™ (Collaborative Biochemical Products, Bedford, MA) in 1:1 (v/v) nutrient mixture F-12 and Dulbecco's modified Eagle's medium (DMEM) (3 ml/well) supplemented with growth factors as described (29, 30). Cultures were incubated in a humidified atmosphere of 95% air and 5% CO_2 (v/v) at 35 °C. After 48 h of incubation, cultures were hypotonically treated with 20 mM Tris (pH 7.4) for 2.5 min to lyse residual germ cells (31), followed by two successive washes with nutrient mixture F-12/DMEM to remove cell debris. The media were replaced every 24 h. The purity of these Sertoli cell cultures was routinely analyzed by electron and light microscopy (32, 33) as well as by reverse transcription-PCR as described (34). Sertoli cells cultured for 5 days were either lysed in SDS lysis buffer (0.125 M Tris (pH 6.8) at 22 °C containing 1% (w/v) SDS, 2 mM EDTA, 2 mM *N*-ethylmaleimide, 2 mM phenylmethylsulfonyl fluoride, 1.6% (v/v) 2-mercaptoethanol, 1 mM sodium orthovanadate, and 0.1 μM sodium okadate) for immunoblotting experiments or used for Sertoli-germ cell co-cultures.

Germ Cell Isolation—Germ cells were isolated from 90-day-old rat testes by a mechanical procedure (35), except that elongating/elongated spermatids were not removed by omitting the glass wool filtration step. Isolated germ cells were incubated with 1 μM gelsolin (Sigma) in nutrient mixture F-12/DMEM for 15 min to disrupt residual actin cytoskeleton in the ES structure that might remain associated with elongating/elongated spermatids. This concentration was selected based on a previous study (36). The purity of germ cells was >95% when examined microscopically and assessed by other criteria (34). Germ cells were either lysed in SDS lysis buffer for immunoblotting or used for Sertoli-germ cell co-cultures within 1 h after isolation.

Sertoli-Germ Cell Co-cultures—Germ cells isolated from adult rat testes were added onto the Sertoli cell epithelium on day 6 after the Sertoli cells had been cultured alone for 5 days, forming an intact epithelium (32), and co-cultured at a Sertoli/germ cell ratio of 1:1 to permit ES assembly. Time 0 represents the time at which germ cells were added onto the Sertoli cell epithelium. Co-cultures were terminated at specific time points by SDS lysis buffer for immunoblotting or by cell lysis buffer (20 mM Tris (pH 7.5) containing 150 mM NaCl, 1 mM EDTA, 1 mM EGTA, 1% (v/v) Triton X-100, 2.5 mM sodium pyrophosphate, 1 mM β-glycerol phosphate, 1 mM sodium orthovanadate, 1 μg/ml leupeptin, and 1 mM phenylmethylsulfonyl fluoride) for kinase assay. Using this approach, any changes in target proteins or intrinsic kinase activity could be ascribed to the assembly of Sertoli-germ cell anchoring junctions (*viz.* apical ES and desmosome-like junctions) because basal ES and tight junctions (TJs) had already been established when Sertoli cells were cultured alone for 5 days.

Seminiferous Tubule Cultures—Seminiferous tubules were isolated from the testes of adult rats (~300 g of body weight) with negligible

TABLE I

Sources of antibodies and the working dilutions that were used for different experiments in this study

Antibody	Vendor	Catalog no.	Uses[a]
Mouse anti-PI3K p85α	Santa Cruz Biotechnology Inc. (Santa Cruz, CA)	sc-1637	WB (1:400), IP, IH (1:50), IF (1:50)
Rabbit anti-PI3K p110α	Cell Signaling Technology, Inc. (Beverly, MA)	4254	WB (1:1000)
Mouse anti-PTEN	Cell Signaling Technology, Inc.	9556	WB (1:1000), IP, IH (1:50)
Rabbit anti-PKB	Cell Signaling Technology, Inc.	9272	WB (1:1000), IP, IH (1:50)
Rabbit anti-phospho-PKB Thr^{308}	Cell Signaling Technology, Inc.	4056	WB (1:1000)
Rabbit anti-phospho-PKB Ser^{473}	Cell Signaling Technology, Inc.	9271	WB (1:1000)
Rabbit anti-phospho-PKB Ser^{473}	Cell Signaling Technology, Inc.	9277	IH (1:50), IF (1:50)
Rabbit anti-PDK1	Cell Signaling Technology, Inc.	3062	WB (1:1000), IP
Rabbit anti-αPAK	Santa Cruz Biotechnology Inc.	sc-881	WB (1:400), IP, IH (1:50)
Rabbit anti-ERK1/2	Cell Signaling Technology, Inc.	9102	WB (1:1000)
Rabbit anti-phospho-ERK1/2	Cell Signaling Technology, Inc.	9101	WB (1:1000)
Rabbit anti-PLCγ^{b}	Santa Cruz Biotechnology Inc.	sc-81	WB (1:400)
Mouse anti-β1-integrin	BD Transduction Laboratories (San Jose, CA)	610468	IP
Rabbit anti-FAK	Santa Cruz Biotechnology Inc.	sc-558	IP
Rabbit anti-phospho-FAK Tyr^{397}	Upstate Biotechnology, Inc. (Lake Placid, NY)	07–012	IP
Mouse anti-paxillin	BD Transduction Laboratories	P13520	IP
Mouse anti-p130^{Cas}	BD Transduction Laboratories	P27820	IP
Mouse anti-vinculin	Sigma	V9193	IP
Mouse anti-gelsolin	BD Transduction Laboratories	610412	IP
Mouse anti-N-cadherin	Zymed Laboratories Inc. (San Francisco, CA)	33-3900	IP
Goat anti-nectin-3	Santa Cruz Biotechnology Inc.	sc-14806	IP
Goat anti-actin	Santa Cruz Biotechnology Inc.	sc-1616	WB (1:200)
Mouse anti-vimentin	Santa Cruz Biotechnology Inc.	sc-6260	WB (1:400)
Mouse anti-α-tubulin	Santa Cruz Biotechnology Inc.	sc-8035	WB (1:400)

[a] WB, Western blotting or immunoblotting; IP, immunoprecipitation; IH, immunohistochemistry; IF, immunofluorescence microscopy. The working dilutions are indicated in parentheses, except for IP, for which a working dilution of 1:100 was used.

[b] PLCγ, phospholipase Cγ.

Leydig cell contamination (37). Lysates were obtained by homogenizing tubules in immunoprecipitation buffer (0.125 M Tris (pH 6.8) at 22 °C containing 1% (v/v) Nonidet P-40, 2 mM EDTA, 2 mM *N*-ethylmaleimide, 2 mM phenylmethylsulfonyl fluoride, 1 mM sodium orthovanadate, and 0.1 μM sodium okadate).

Effects of Chelating Agents (e.g. EGTA and EDTA), Vanadate, and the Epidermal Growth Factor (EGF) on Protein Kinases and Intrinsic PKB Activity—Because several studies have reported that EDTA can interact with vanadate via chelation (39–43), thereby reducing the free concentration of vanadate in the sample buffer and thus limiting the inhibitory effect of vanadate on protein-tyrosine phosphatases, we performed some of the experiments either (i) by substituting EDTA (2 mM; note that EDTA is widely used in buffers for studying protein phosphorylation, including those obtained commercially) with EGTA (2 mM) in lysis buffers because this latter chelating agent has been shown to form a much weaker complex with vanadate (43) or (ii) by replacing EDTA or EGTA that served as a metalloprotease inhibitor in the buffer with 2 mM 1,10-phenanthroline (a metalloprotease inhibitor) and compared the results with lysis buffers containing EDTA. This applied to different buffers used in this study, including the cell lysis buffer to be used for intrinsic kinase assay (see below). On this note, we anticipated that endogenous protein-tyrosine phosphatase inhibitors could protect samples from unwanted activities of protein-tyrosine phosphatase; however, a complete blockade of protein-tyrosine phosphatase could shift the base line of the intrinsic kinase activity, but plausibly *not* the trend of activation. Furthermore, EGF (a well known receptor protein-tyrosine kinase), which was present in the Sertoli cell cultures at 2.5 ng/ml as a growth factor in our experiments as described previously (44, 45), has recently been shown to stimulate Sertoli cell ERK activity at 100 ng/ml (46, 47). As such, additional controls were included in Sertoli-germ cell co-cultures in which EGF was omitted in the spent nutrient mixture F-12/DMEM. We expected that the endogenous ERK and phospho (p)-ERK basal levels in co-cultures containing EGF would be higher than in those without EGF; however, its presence plausibly would not interfere with the trend of p-ERK1/2 activation during AJ assembly.

Treatment of Rats with AF-2364 to Induce Germ Cell Loss from the Seminiferous Epithelium—AF-2364 (1-(2,4-dichlorobenzyl)-1*H*-indazole-3-carbohydrazide) was synthesized to a purity of >99.8% as described (48). This compound has been shown to perturb Sertoli-germ cell adhesion function to induce premature loss of germ cells from the epithelium, causing reversible infertility in rats (48, 49). One of the apparent targets of AF-2364 is the apical ES without affecting the BTB integrity (3). Adult rats weighing 250–300 g were fed one dose of AF-2364 at 50 mg/kg of body weight. The time when the rats were fed AF-2364 was designated time 0 (control). Thereafter, rats were housed separately for 15 days. Testes were removed at specified time points from a group of three rats for each time point. For immunoblotting, testes were homogenized for lysate preparation either in SDS lysis buffer (for immunoblotting) or in cell lysis buffer (for PKB intrinsic kinase assay). For immunohistochemistry, testes were immediately fixed in 4% paraformaldehyde for paraffin embedding.

Electron Microscopy—Electron microscopy was performed to examine the functional ES structures found in Sertoli-germ cell co-cultures, which were terminated 48 h after addition of germ cells to the Sertoli cell epithelium, as described previously (50).

Immunoblotting—Protein concentration was estimated by Coomassie Blue dye binding assay using bovine serum albumin as a standard (51). Proteins (~100 μg from each sample within an experimental group) were resolved by SDS-PAGE (7.5 or 12.5% T) under reducing conditions (52). Proteins were electroblotted onto nitrocellulose membranes and immunostained. All primary antibodies were shown to cross-react with the corresponding target proteins in rats as indicated by the manufacturers (Table I). Depending on the origin of the primary antibody, one of the following horseradish peroxide-conjugated secondary antibodies was used: bovine anti-rabbit IgG, bovine anti-goat IgG, or goat anti-mouse IgG. Target proteins in the blots were visualized using an ECL kit (Amersham Biosciences).

Co-immunoprecipitation (Co-IP)—Co-IP was performed as described previously (8, 34). Lysates of testes and/or seminiferous tubules that were not incubated with any antibodies or that were incubated with normal serum served as controls. All primary antibodies used for immunoprecipitation were shown to cross-react with the corresponding target proteins in rats as indicated by the manufacturers (Table I).

PKB Kinase Assay—The intrinsic PKB activity during anchoring junction assembly in Sertoli-germ cell co-cultures and during AF-2364-induced Sertoli-germ cell anchoring junction disruption in the testis was analyzed using kits purchased from Cell Signaling Technology, Inc. (catalog no. 9840) according to the protocols provided by the manufacturer. In brief, lysates of Sertoli-germ cell co-cultures (~200 μg of protein) and AF-2364-treated testes (~200 μg of protein) were prepared as described above and immunoprecipitated using immobilized anti-PKB antibody. Immunocomplexes were incubated in kinase buffer containing the glycogen synthase kinase-3 (GSK-3) fusion protein (~30 kDa), which is the putative substrate of PKB, in the presence of ATP. Phosphorylation of GSK-3 was quantified using anti-p-GSK-3α/β antibody by immunoblotting and detected with a chemiluminescence kit (Amersham Biosciences).

Immunohistochemistry—Streptavidin/biotin-conjugated peroxidase immunostaining was performed as described previously (8, 38) using Histostain™ SP kits (Zymed Laboratories Inc.). Testes were fixed in 4% paraformaldehyde in phosphate-buffered saline (PBS) for 24 h, dehy-

drated, embedded in paraffin, and sectioned. After deparaffinization and rehydration, antigen unmasking was performed by heating sections in 10 mM sodium citrate buffer (pH 6.0) for 10 min at a temperature at or just below boiling. Sections were then cooled at room temperature for 20 min, followed by treatment with 3% (v/v) hydrogen peroxide in methanol for 20 min. To minimize nonspecific binding, sections were incubated with serum blocking solution (Zymed Laboratories Inc.) and subsequently incubated overnight with primary antibodies in a moist chamber at 35 °C. Mouse anti-PI3K, mouse anti-PTEN, rabbit anti-PKB, rabbit anti-p-PKB Ser^{473}, and rabbit anti-αPAK primary antibodies were used (Table I). Thereafter, sections were incubated with biotinylated goat anti-mouse IgG or goat anti-rabbit IgG for 30 min, followed by streptavidin-conjugated peroxidase for 10 min. Color development was performed using an aminoethylcarbazole mixture, and sections were counterstained in hematoxylin and mounted. Sections were examined and photographed using an Olympus BX40 microscope. All micrographs were digitally acquired. At least 50–100 sections were examined from each testis, and at least three rats from each time point were examined. Controls consisted of sections incubated with (i) normal mouse or rabbit serum instead of the primary antibodies, (ii) PBS instead of the primary antibodies, (iii) normal mouse or rabbit serum in place of the secondary antibodies, and (iv) primary antibodies that had been pre-absorbed with lysates of seminiferous tubules or control peptides provided by the manufacturer. To minimize interexperimental variations, all sections of testes within a treatment group (*e.g.* AF-2364 treatment with and without wortmannin or anti-β1-integrin IgG pretreatment) were processed simultaneously with three to four sections/slide so that two to four slides were subjected to antibody incubation and color development in a single experimental session. Each experiment was repeated at least three to four times, and the results shown herein are representations of these analyses.

Immunofluorescence Microscopy—Fluorescence microscopy was performed essentially as described previously (8, 34, 38). In brief, testes were fixed in Bouin's fixative (4% formaldehyde in picric acid), embedded in paraffin, and sectioned. Following removal of the paraffin, sections were incubated with serum blocking solution. Sections were subsequently incubated with mouse anti-PI3K antibody, followed by fluorescein isothiocyanate-labeled goat anti-mouse IgG. Thereafter, sections were washed with PBS and incubated with rabbit anti-PKB Ser^{473} antibody, followed by Cy3-labeled goat anti-rabbit IgG, and then mounted in Vectashield™ (Vector Laboratories, Burlingame, CA). Fluorescence microscopy was performed using an Olympus BX40 microscope equipped with Olympus UPlanF1 fluorescence optics. All images were digitally acquired and analyzed as described above.

Treatment of Rats with Wortmannin—To assess the effect of wortmannin (M_r 428.4; catalog no. 681675, Calbiochem), a PI3K-specific inhibitor (53), on AF-2364-induced anchoring junction disruption, one testis from each rat ($n = 3$) was injected with wortmannin (0.5 μM; assuming a testicular volume of ~1.6 ml/testis, 0.8 nmol (~0.3427 μg) of wortmannin was used per testis) prior to AF-2364 treatment (50 mg/kg of body weight) by gavage at two sites with ~100 μl/site as described (38). Wortmannin was prepared in Me_2SO (1 mg/ml) and diluted in 200 μl of saline to the desired concentration. The same concentration of Me_2SO alone diluted in 200 μl of saline was injected into the other testis of each rat (vehicle control). Rats were killed on days 2, 4, and 6, and testes were removed, frozen in liquid nitrogen, and stored at −80 °C. Sections were obtained in a cryostat and stained with Mayer's hematoxylin. Cross-sections of testes were randomly selected, and seminiferous tubules consisting of elongating/elongated spermatids were scored as described (38). At least 100 tubules selected randomly from each testis were photographed, digitally processed, and printed for scoring, and at least three testes from different rats were examined and scored. A tubule from rats treated with AF-2364, inhibitor + AF-2364, or inhibitor alone that contained <50% of elongating/elongated spermatids *versus* control tubules (for control testes, the number of elongating/elongated spermatids in a typical cross-section of a seminiferous tubule at stages I–VI, VII and VIII, and XI–XIV was ~129 ± 17, 143 ± 13, 112 ± 12, respectively, and elongating/elongated spermatids were not found in stage IX and X tubules) was scored as one tubule with significant loss of elongating/elongated spermatids from the epithelium. The percentage of seminiferous tubules (ST) with normal elongating/elongated spermatids after treatment with AF-2364, AF-2364 + inhibitor, or inhibitor alone was calculated as follows: $(ST_{\text{AF-2364 with/without inhibitor}}/ST_{\text{control}}) \times 100\%$.

Blocking Integrin Function Using Anti-β1-integrin IgG Administered Intratesticularly to Assess Its Subsequent Effects on AF-2364-induced Spermatid Loss from the Seminiferous Epithelium—To further validate the involvement of the α6β1-integrin·laminin γ3 protein complex and the downstream FAK signaling pathway in mediating Sertoli-germ cell adhesion function, rats ($n = 3$ per time point in each treatment group) received anti-β1-integrin IgG (50 μg/testis) (Table I) or mouse IgG (50 μg/testis) diluted in PBS to 200 μl on the left testis at two sites at 100 μl/site as described (38). Mouse IgG was isolated using normal mouse serum (~5 ml) by sequential ammonium sulfate precipitation and DEAE affinity chromatography as described (54). The right testis of the same rat, serving as the corresponding control, received either PBS or no treatment. Thereafter, rats were treated with a single dose of AF-2364 (50 mg/kg of body weight) by gavage and killed on days 6 and 15. Testes were fixed in Bouin's fixative, embedded in paraffin, sectioned, and stained by hematoxylin and eosin to assess spermatid loss from the seminiferous epithelium. Tubules containing no elongating/elongated spermatids were scored as "damaged" tubules because by days 6 and 15, >90% of the tubules (except for the group pretreated with anti-β1-integrin antibody) contained no elongating/elongated spermatids. In normal testes, only stage IX and X tubules contained no elongating/elongated spermatids, which represented ~5% of all the tubules, and these tubules contained several layers of round spermatids in the epithelium, which could be readily identified. About 100 tubules were examined and scored randomly from each testis, and at least three testes from different rats were scored. The percentage of tubules with elongating/elongated spermatids was estimated using the formula given above.

Statistical Analysis—Multiple comparisons were performed using one-way analysis of variance, followed by Tukey's HSD test to compare selected pairs of experimental groups, so that changes in the level of a target protein kinase at a selected time point within an experimental group could be compared between samples. In selected experiments, Student's *t* test was also performed by comparing treatment groups with the corresponding controls. Statistical analysis was performed using the GB-STAT statistical analysis software package (Version 7, Dynamic Microsystems, Inc., Silver Spring, MD).

RESULTS

Functional Apical and Basal ES Structures, Desmosome-like Junctions, TJs, and the BTB in Sertoli-Germ Cell Co-cultures in Vitro

In co-culture experiments, Sertoli cells were initially cultured alone at 0.5×10^6 cells/cm^2 on Matrigel-coated dishes for 5 days to form an intact cell epithelium with functional basal ES structures and TJs, which in turn constituted the functional BTB (Fig. 1). Thereafter, germ cells isolated from adult rat testes were plated onto this cell epithelium, and functional ES structures and desmosome-like junctions were detected within 24–48 h (Fig. 1). Fig. 1*A* illustrates a functional desmosome-like junction structure between a germ cell and a Sertoli cell (see *boxed area* in Fig. 1*A* enlarged in Fig. 1*B*). Sertoli cells in culture were typified by the presence of microvilli (see *asterisks* in Fig. 1, *A–C*, *E*, and *F*), which engulfed the adhering germ cells. A functional desmosome-like junction was characterized by the presence of electron-dense substances as patches on both sides of the Sertoli and germ cell plasma membranes (Fig. 1, *A* and *B*). Functional apical ES structures were also detected in these co-cultures (Fig. 1, *C* and *D*). The apical ES was characterized by the presence of actin filaments (see *white arrowhead* in Fig. 1*D*) sandwiched between two apposing Sertoli and germ cell membranes and the cisternae of the endoplasmic reticulum, and these structures were detected only on the Sertoli cell side (Fig. 1*D*). The apical ES was also found between an elongating spermatid and the Sertoli cell epithelium (Fig. 1*E*), which was characterized by actin filament bundles sandwiched between the cisternae of the ectoplasmic reticulum and the apposing plasma membranes of Sertoli and germ cells. Functional BTB structures were also detected in the Sertoli cell epithelium (Fig. 1, *F* and *G*). The BTB was typified by the presence of basal ES and TJs (see *black arrowheads* in Fig. 1*G*). The basal ES was characterized by the presence of actin filament bundles (see *white arrowhead* in Fig. 1*G*) sandwiched

balt3/zbc-bc/zbc02805/zbc1105-05g saylora S=4 16/5/05 15:32 4/Color Figure(s) 4-7,10,11,13 ARTNO: M501049200

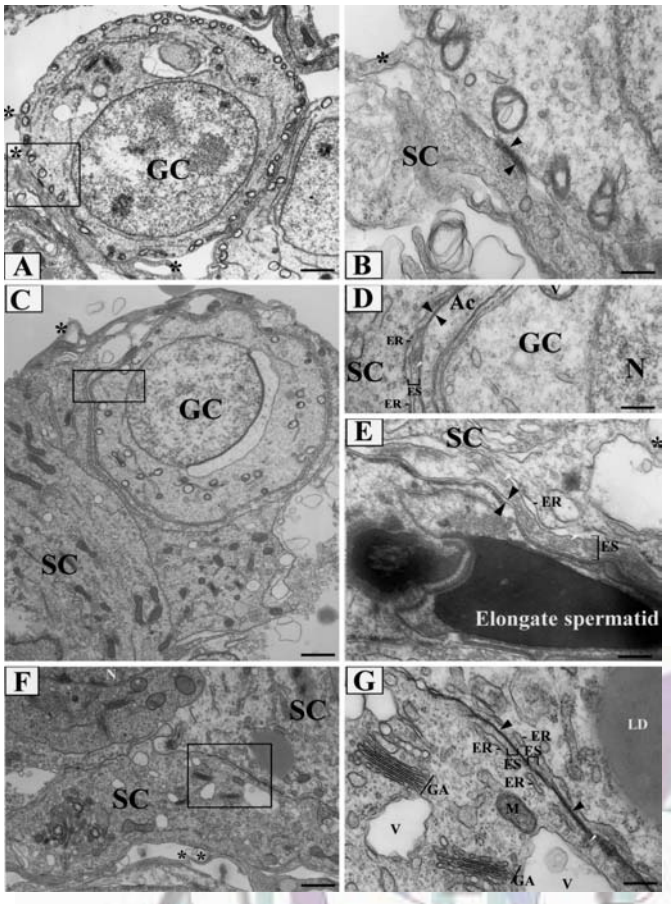

F2

FIG. 1. **Functional cell-cell intermediate filament-based desmosome-like junctions and cell-cell actin-based ES structures at the Sertoli-germ (apical ES) and Sertoli-Sertoli (basal ES) cell interfaces in Sertoli-germ cell co-cultures *in vitro* as assessed by electron microscopy.** Sertoli-germ cell co-cultures were prepared as described under "Experimental Procedures." In brief, germ cells isolated from adult rat testes were plated onto the Sertoli cell epithelium on day 6 to initiate Sertoli-germ cell anchoring junction assembly after these Sertoli cells had been cultured alone for 5 days to form an intact epithelium. These co-cultures were terminated and processed for electron microscopy 2 days thereafter. Electron micrographs of the functional desmosome-like junction between a Sertoli cell and a spermatocyte are shown in *A* and *B*. The *boxed area* in *A* was enlarged and is shown in *B*. The *arrowheads* illustrate the electron-dense material lying alongside the two apposing Sertoli cell (*SC*) and germ cell (*GC*) membranes typical of desmosome-like junctions. The *asterisks* represent the microvilli of Sertoli cells engulfing the germ cell, a feature common to Sertoli cells when cultured *in vitro*. Electron micrographs of the functional apical ES between a Sertoli cell and a step 8 spermatid are shown in *C* and *D*. The *asterisk* indicates a microvillus, which is a typical feature of Sertoli cells cultured *in vitro*. The *boxed area* in *C* is enlarged in *D* and illustrates the typical feature of the apical ES. A typical apical ES structure between a Sertoli cell (see microvillus indicated by the *asterisk*) and an elongating spermatid is shown in *E*. The ES is morphologically characterized by the presence of distinctive bundles of actin filaments (*white arrowheads*) sandwiched between the plasma membrane of the Sertoli cell and the cisternae of the endoplasmic reticulum (*ER*). The apposing *black arrowheads* represent the two apposing plasma membranes of Sertoli and germ cells. In the apical ES, the actin filament bundles and the endoplasmic reticulum are restricted only to the Sertoli cell side (*C–E*), which is in contrast to the basal ES at the BTB site shown in *F* and *G* because these structures (*i.e.* actin filament bundles (*white arrowheads*) sandwiched between the Sertoli cell plasma membrane and the cisternae of the endoplasmic reticulum) are found on both sides of the two apposing Sertoli cells. Furthermore, basal ES are present side-by-side with TJs (see *black arrowheads* in *G*), which in turn constitute the BTB, which is clearly visible in this co-culture between two adjacent Sertoli cells (*F* and *G*). For instance, the microvilli (*asterisks*) typical of Sertoli cells cultured *in vitro* were found and can be seen in *F*. *V*, vacuole. *Scale bars* = 3 μm (*A*, *C*, and *F*), 0.5 μm (*B*), 0.6 μm (*D*), 0.2 μm (*E*), and 0.75 μm (*G*).

AQ: NN

AQ: R

between the Sertoli cell membrane and the cisternae of the endoplasmic reticulum. The differences between the basal ES (Fig. 1*G*) and apical ES (Fig. 1, *D* and *E*) are that the ES structures in the basal ES were found on both sides of two apposing Sertoli cells, near the plasma membrane, and the interface of the two Sertoli cells at the basal ES was always filled with TJs (Fig. 1, *G versus D*), which in turn constituted the BTB. In brief, electron microscopy analyses revealed that typical structures of the functional BTB, desmosome-like junctions, and basal and apical ES were found in these co-cultures, illustrating that this is a novel model to study junction dynamics *in vitro*.

Relative Protein Levels of PI3K p85α, PI3K p110α, PTEN, PDK1, PKB, p-PKB Thr^{308}, p-PKB Ser^{473}, PAK, ERK, p-ERK, and Phospholipase Cγ in Sertoli and Germ Cells

To determine the endogenous levels of different target proteins (*viz.* protein kinases) pertinent to ES regulation in Sertoli and germ cells, protein lysates were obtained from 20-day-old Sertoli cells cultured for 5 days alone (Fig. 2*A*, *left panel*, *20D SC*) and from total germ cells isolated from 90-day-old rats that were used within 2 h (*90D GC*). All of the target proteins were detected in both Sertoli and germ cells, except for PDK1, which was found only in germ cells. The protein levels of PI3K p85α, PI3K p110α, and PTEN were higher in 90-day-old germ cells than in 20-day-old Sertoli cells, whereas PKB, p-PKB Ser^{473} (the activated phosphorylated form of PKB), PAK, ERK, p-ERK, and phospholipase Cγ were more predominant in 20-day-old Sertoli cells (Fig. 2*A*, *left panel*). Only p-PKB Thr^{308} (the activated phosphorylated form of PKB) had a relatively similar protein level in both Sertoli and germ cells (Fig. 2*A*).

Changes in the Endogenous Levels of Different Protein Kinases and the Intrinsic Kinase Activity of PKB during Anchoring Junction Assembly in Sertoli-Germ Cell Co-cultures

To examine the involvement of PI3K and its downstream signaling molecules in Sertoli-germ cell anchoring junction (*e.g.* apical ES) assembly, protein lysates obtained from co-cultures were subjected to immunoblotting to investigate any changes in these signaling molecules. Indeed, induction of the protein levels of PI3K p85α, PI3K p110α, PDK1, p-PKB Thr^{308}, p-PKB Ser^{473}, PAK2, and p-ERK (Fig. 2, *A* and *B*) was detected after germ cell addition to the Sertoli cell epithelium at the time of cell attachment, preparing for the establishment of anchoring junctions (32). When functional apical ES structures and desmosome-like junctions were established by 2 days (Fig. 1), many of the protein kinases returned to their basal levels, except for p-ERK, which remained significantly induced for up to 3 days (Fig. 2, *A* and *B*). The protein level of PTEN remained relatively steady at the early time points, but its level tumbled by 1 day and became significantly reduced by 2 and 3 day (Fig. 2, *A* and *B*). The protein levels of PKB, PAK1, and ERK remained relatively unaltered throughout the experiment, whereas phospholipase Cγ exhibited a gradual yet significant decline in its protein level during Sertoli-germ cell anchoring junction assembly (Fig. 2, *A* and *B*). More important, the induced p-PKB Thr^{308} and p-PKB Ser^{473} levels were also accompanied by a significant increase in intrinsic PKB kinase activity (see Fig. 3), which was quantified by an increase in PKB-induced phosphorylation of the GSK-3 fusion protein, which is a putative PKB substrate, as shown in the immunoblot in Fig. 3. Equal protein loading in the kinase assay was assessed by probing an

balt3/zbc-bc/zbc-bc/zbc02805/zbc1105-05g saylora S=4 16/5/05 15:32 4/Color Figure(s) 4-7,10,11,13 ARTNO: M501049200

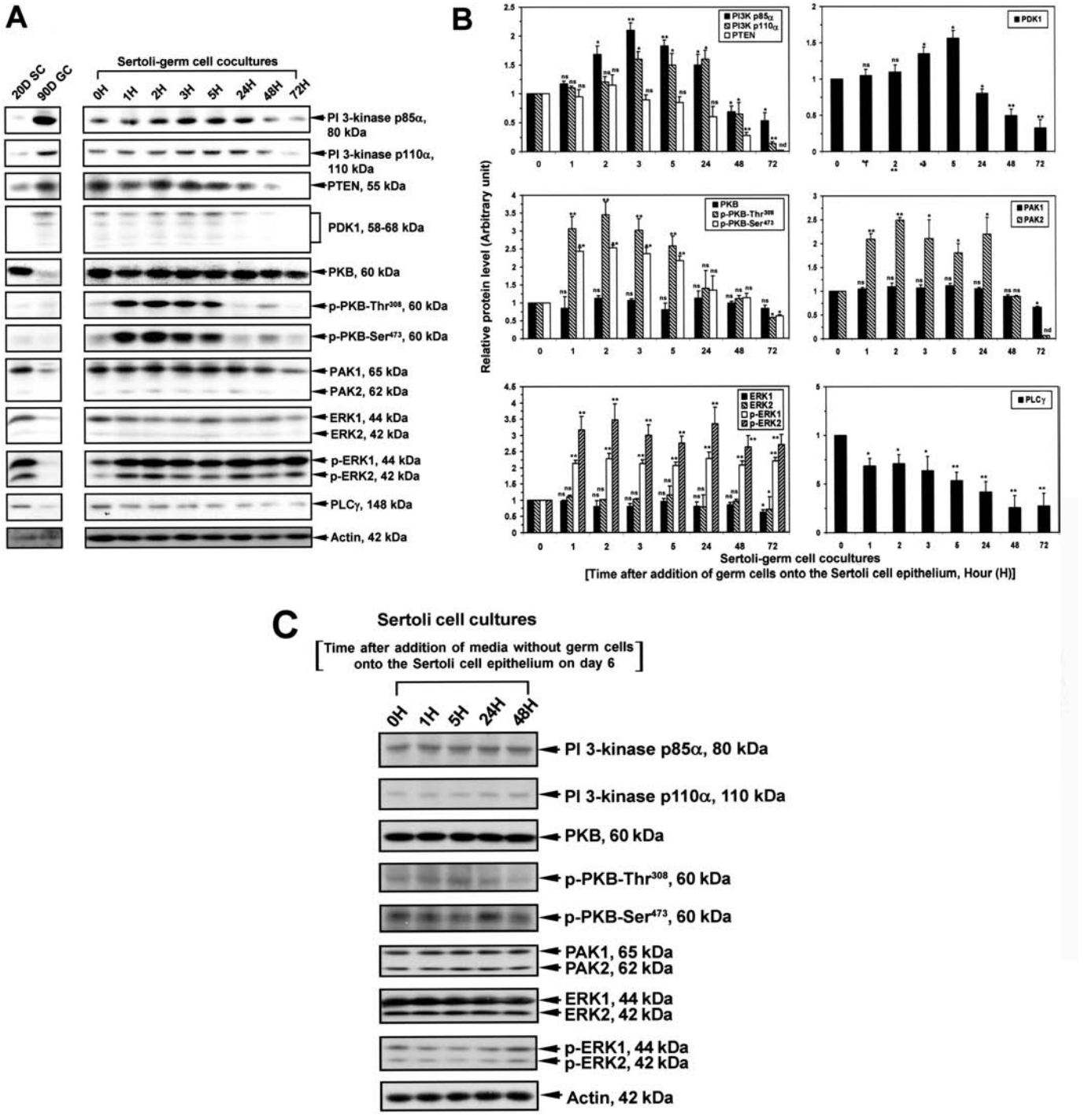

FIG. 2. **Relative protein levels of PI3K p85*α*, PI3K p110*α*, PTEN, PDK1, PKB, p-PKB Thr^{308}, p-PKB Ser^{473}, PAK, ERK, p-ERK, and phospholipase C*γ* in Sertoli and germ cells and their changes in Sertoli-germ cell co-cultures during the assembly of functional anchoring junctions *versus* Sertoli cells cultured alone (control).** Sertoli cells isolated from 20-day-old rats (*20D SC*) were cultured alone for 5 days at 0.5×10^6 cells/cm^2, forming an intact cell epithelium. On day 6, freshly isolated germ cells from 90-day-old rats (*90D GC*) were also isolated. The steady-state protein levels of different target proteins are shown (*A*, *left panel*). These germ cells were then plated onto the Sertoli cell epithelium at a Sertoli cell/germ cell ratio of 1:1 to initiate anchoring junction assembly (*A*, *right panel*; and *B*) *versus* control cultures without germ cell addition (*C*). Co-cultures were then terminated at the specified time points to obtain whole cell lysates for immunoblotting using ~50 μg of total protein/lane (*A*). Densitometric scanning of immunoblots, such as those shown in *A*, was performed in which the level of a target protein was normalized against the protein level at time 0, which was arbitrarily set at 1 (*B*). Each *bar* represents the mean ± S.D. of results from three experiments using different batches of cells. Each experiment had replicate cultures. *, $p < 0.05$, significantly different by analysis of variance; **, $p < 0.01$; *ns*, not significantly different; *nd*, not detectable. *PLC*γ, phospholipase Cγ.

immunoblot with anti-GSK antibody; the same amount of protein used for the intrinsic PKB kinase assay was also used for this blot (see Fig. 3). It is obvious that the changes illustrated in Fig. 2 regarding the activation of different signaling molecules in the PI3K/PKB/ERK signaling pathway can be ascribed to the event of Sertoli-germ cell anchoring junction assembly because when Sertoli cells were cultured alone and terminated between 1 and 48 h, no changes in the steady-state PI3K, p-PKB, PAK1/2, and p-ERK1/2 protein levels were detected (Fig. 2*C*).

balt3/zbc-bc/zbc-bc/zbc02805/zbc1105-05g saylora S=4 16/5/05 15:32 **4/Color Figure(s) 4-7,10,11,13** ARTNO: M501049200

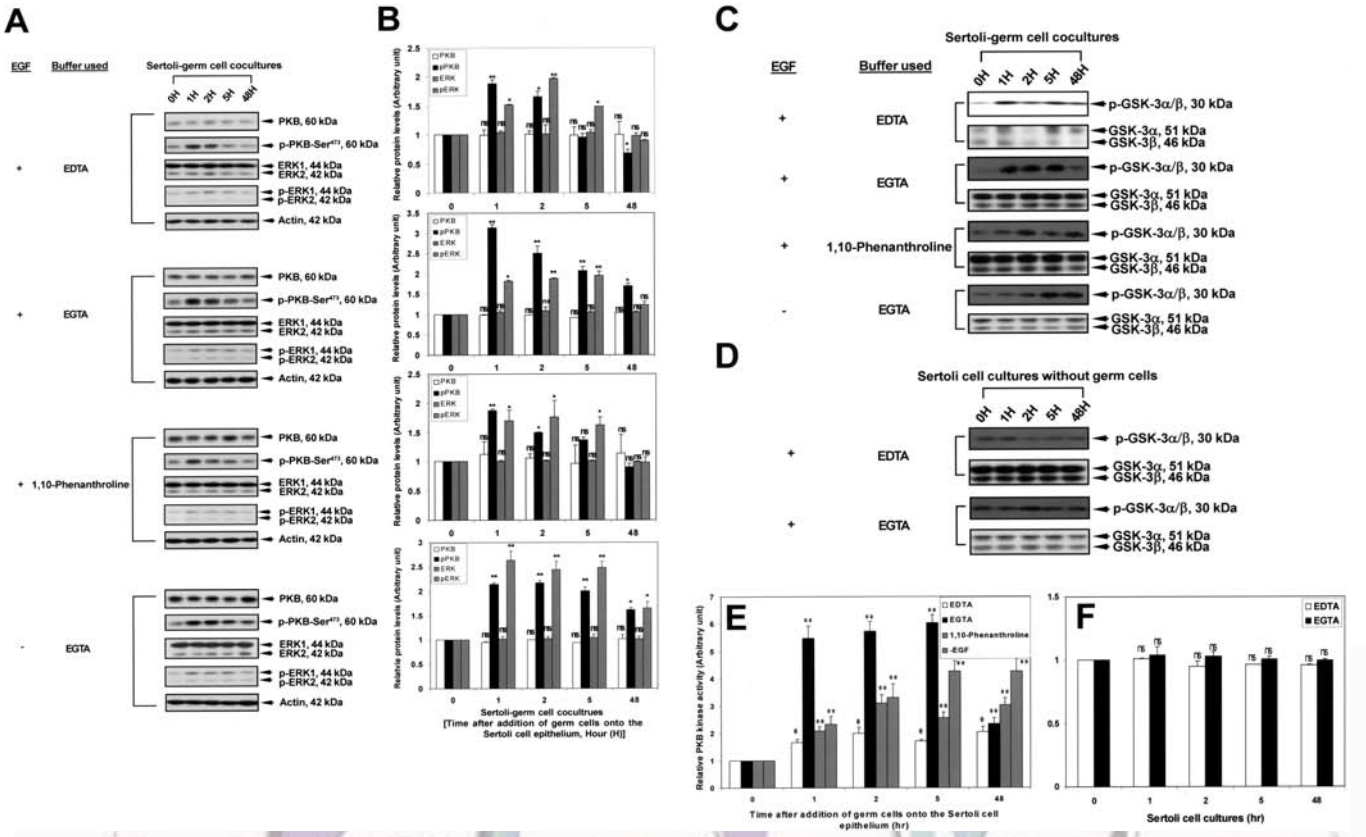

FIG. 3. **Effects of chelating agents (*e.g.* EDTA and EGTA), a metalloprotease inhibitor (*e.g.* 1,10-phenanthroline), and EGF on induction of p-PKB, p-ERK, and intrinsic PKB activity during Sertoli-germ cell anchoring junction assembly *in vitro*.** *A*, Sertoli cells were cultured alone for 5 days at 0.5×10^6 cells/cm^2 to form an intact epithelium. On day 6, germ cells isolated from adult rat testes were plated onto the Sertoli cell epithelium at a Sertoli cell/germ cell ratio of 1:1 to initiate anchoring junction assembly. Cultures with (+) and without (−) EGF (2.5 ng/ml; including daily replacement of nutrient mixture F-12/DMEM at time 0 when Sertoli cells were isolated and plated onto Matrigel-coated dishes) were terminated at 0 (*i.e.* terminated immediately after germ cell addition to the Sertoli cell epithelium), 1, 2, 5, and 48 h using lysis buffer containing EDTA (2 mM), EGTA (2 mM), or 1,10-phenanthroline (2 mM). About 50 μg of protein was used per lane, and different target proteins (PKB, p-PKB-Ser^{473}, ERK1/2, and p-ERK1/2) were quantified by immunoblotting. The same blot was stripped and reprobed with anti-actin antibody to assess equal protein loading and uniform protein transfer from gels to the nitrocellulose membrane. *B*, densitometric scanning of immunoblots, such as those shown in *A*, was performed, and the results were normalized against actin. The level of each target protein at each time point was compared with its level at time 0, which was arbitrarily set at 1. Each *bar* is the mean ± S.D. of three determinations. The bars for ERK and p-ERK represent the summation of ERK1/2 and p-ERK1/2, respectively. *C*, ~200 μg of protein from each sample within an experimental group was used for the PKB intrinsic activity assay as described under "Experimental Procedures"; the lysis buffer contained EDTA, EGTA, or 1,10-phenanthroline with or without EGF (2.5 ng/ml) in nutrient mixture F-12/DMEM. *D*, this is the control experiment of *C* in which germ cells were not plated onto the Sertoli cell epithelium on day 6 (*i.e.* Sertoli cells alone), but were terminated at the same time period as shown in *C*. The PKB activity in each sample following a pull-down assay (see "Experimental Procedures") was quantified by its ability to phosphorylate the 30-kDa GSK fusion protein provided in the assay kit, which was detected using anti-p-GSK-3α/β antibody by immunoblotting (*C* and *D*). The endogenous GSK-3α (51 kDa) and GSK-3β (46 kDa) levels in the protein lysates from co-cultures used for PKB intrinsic activity assay were quantified by immunoblotting using anti-GSK-3$\alpha/3\beta$ antibody, which also served as a protein loading control (*C* and *D*). *E* and *F*, these histograms illustrate the corresponding densitometrically scanned results of *C* and *D*. Each *bar* is the mean ± S.D. of three determinations. The protein level at time 0 was arbitrarily set at 1, and data were normalized against the total GSK-3α/β level. *, $p < 0.05$, significantly different by analysis of variance; **, $p < 0.01$; *ns*, not significantly different.

Effects of Different Chelating Agents (e.g. EDTA and EGTA) and EGF on Protein Kinases and Intrinsic PKB Activity in Sertoli-Germ Cell Co-cultures during Anchoring Junction Assembly

EDTA was used as a chelating agent in the lysis buffers to block metalloprotease activities (*e.g.* MMP-2 and MMP-9, which are also products of Sertoli cells). However, its chelating effects on vanadate limit the action of sodium orthovanadate (39, 41, 42), which was also included in the buffers to block protein-tyrosine phosphatases in testis lysates to study protein kinases. A recent study has cautioned against the use of EDTA in studies investigating the functions of phosphoproteins (*e.g.* protein and lipid kinases), including numerous commercial assay and buffer kits (42). To address this important issue, a series of studies was conducted, and the results are shown in Fig. 3. Although the presence of EDTA did not interfere with the trend regarding induction of p-PKB or p-ERK1/2 during Sertoli-germ cell anchoring junction assembly (Fig. 3, *A* and *B* (*first panels*) *versus* Fig. 2, *A* and *B*) possibly because there were endogenous protein-tyrosine phosphatase inhibitors in the testis lysates, its presence indeed lowered the overall levels of protein kinases (*e.g.* p-PKB and p-ERK1/2) that were induced during anchoring junction assembly (Fig. 3, *A* and *B*). For example, the use of EGTA instead of EDTA in the lysis buffers, which was shown to form a much weaker complex with vanadate (43), resulted in an increase in p-PKB-Ser^{473} of almost 3.2-fold *versus* 1.8-fold (with EDTA) by 1 h during Sertoli-germ cell anchoring junction assembly (Fig. 3, *A* and *B*, *first* and *second panels*). These differences were even more pronounced when the intrinsic PKB activity was monitored (Fig. 3, *C* and *E*). For instance, when EGTA was included in the buffers to block metalloproteases and to permit sodium orthovanadate to exert its effects as a protein-tyrosine phosphatase inhibitor, an ~6-fold increase in PKB activity was detected between 1

AQ: S
AQ: T
AQ: U
F3

balt3/zbc-bc/zbc02805/zbc1105-05g saylora S=4 16/5/05 15:32 4/Color Figure(s) 4-7,10,11,13 ARTNO: M501049200

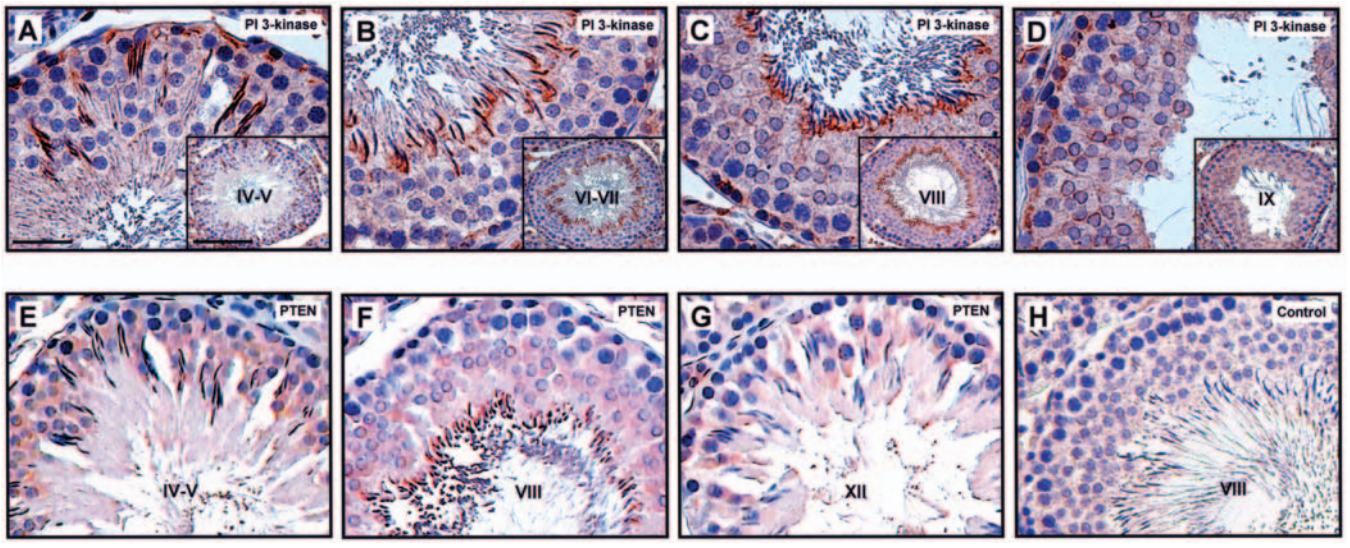

AQ: OO FIG. 4. **Micrographs of cross-sections of adult rat testes showing immunoreactive PI3K (*A–D*) and PTEN (*E–G*) in the seminiferous epithelium at different stages of the epithelial cycle.** *A–D*, representative cross-sections of tubules at stages IV and V, VI and VII, VIII, and IX, respectively, of the epithelial cycle; *E–G*, representative cross-sections of tubules at stages IV and V, VIII, and XII, respectively. Immunoreactive PI3K and PTEN appear as reddish brown precipitates . The *insets* in *A–D* are selected regions of the seminiferous epithelium at lower magnification. *H*, corresponding control testis; sections were incubated with normal mouse IgG instead of primary antibodies. *Scale bar* = 20 μm in *A*, which applies to *B–H*; *scale bar* = 100 μm in the *inset* in *A*, which applies to the *insets* in *B–D*.

and 5 h at the time of Sertoli-germ cell AJ assembly *versus* a 2-fold increase in PKB intrinsic activity with EDTA in the buffers (Fig. 3, *C* and *E*). If 1,10-phenanthroline was used as a metalloprotease inhibitor instead of a chelating agent in the lysis buffers to block metalloprotease activity in testis lysates, the overall steady-state p-PKB and p-ERK1/2 protein levels and the intrinsic PKB activity, in particular, during Sertoli-germ cell anchoring junction assembly were also higher than when EDTA was included in the buffers (Fig. 3, *A–C* and *E*). Furthermore, the presence of EGF (2.5 ng/ml) could indeed interfere with the PKB/ERK signaling function, consistent with two previous reports showing that EGF is a putative ERK activator (46, 47). For instance, if EGF was omitted from the spent medium and EDTA was replaced with EGTA in the lysis buffer, the overall intrinsic PKB activity was lowered compared with co-cultures with EGF at 2.5 ng/ml plus EGTA in the lysis buffer (Fig. 3, *C* and *E*), illustrating that EGF can activate the PKB/ERK signaling pathway, potentiating p-PKB/p-ERK activation during anchoring junction assembly. Perhaps the most important of all, regardless of whether EDTA or EGTA was used as the chelating agent in the lysis buffer, induction of intrinsic PKB activity was *not* detected in Sertoli cells cultured alone without germ cells to initiate anchoring junction assembly, as shown in Fig. 3 (*D* and *F*). Nonetheless, the results shown in Fig. 3 (*A–F*) clearly illustrate that, in future studies, EGTA instead of EDTA should be used in the lysis buffer or the chelating agent should be replaced with 1,10-phenanthroline, in particular, if the precise phosphorylation status of a target protein/lipid kinase is being estimated. However, when the data of Figs. 2 and 3 are compared, it is also obvious that the use of EDTA in the lysis buffer, the presence of EGF at 2.5 ng/ml in the spent medium, or both do not negate the fact that the PKB/ERK signaling pathway is indeed activated during Sertoli-germ cell anchoring junction assembly.

Stage Specificity of PI3K p85α, PTEN, PKB, p-PKB Ser^{473}, and PAK in Normal Rat Testes

Localizations of PI3K p85α and PTEN—The results of immunohistochemistry studies to localize PI3K p85α and PTEN in normal rat testes at different stages of the epithelial cycle are shown in Fig. 4 (*A–D* and *E–G*, respectively). Fig. 4*H* is the corresponding negative control for PI3K p85α and PTEN, in which the primary antibodies were substituted with normal mouse serum (1:50) for immunohistochemistry. PI3K p85α was widely distributed in the seminiferous epithelium and was found in both Sertoli and germ cells (Fig. 4, *A–D*), consistent with the immunoblotting data shown in Fig. 2 (*A* and *B*). PI3K p85α was most abundant in the epithelium at the apical ES from stages IV to VIII (Fig. 4, *A–C*), surrounding the heads of elongated spermatids. Very weak PI3K p85α staining was also detected between Sertoli cells and step 8 and 9 spermatids at stage VIII (Fig. 4*C*) and stage IX (Fig. 4*D*), when the apical ES began to form. PI3K p85α was also detected at the basal ES in a stage-specific manner, with stronger staining in stages IV and V (Fig. 4*A*) and stage IX (Fig. 4*D*), but much weaker staining in stages VI–VIII (Fig. 4, *B* and *C*).

In almost all stages of the epithelial cycle, weak staining of PTEN was found associated with Sertoli cells, spermatogonia, spermatocytes, and round spermatids (Fig. 4, *E–G*). However, virtually no staining could be found in elongating spermatids at stages IV and V (Fig. 4*E*) and XII (Fig. 4*G*). Strong PTEN staining was detected at stage VIII, largely surrounding the heads of elongated spermatids adjacent to the seminiferous tubule lumen, just prior to spermiation (Fig. 4*F*). This result (Fig. 4*F*) is consistent with its localization at the apical ES.

Localizations of PKB and p-PKB Ser^{473}—The localizations of immunoreactive PKB and p-PKB Ser^{473} were almost superimposed in the seminiferous epithelia of adult rat testes (Fig. 5). Fig. 5*H* is the corresponding negative control for PKB and p-PKB Ser^{473}, in which antibodies were substituted with the same concentration of normal rabbit IgG for immunohistochemistry. Similar to PI3K p85α, strong staining of PKB (Fig. 5, *A–D*) and p-PKB Ser^{473} (Fig. 5, *I–M*) was observed at the site of apical ES from stages IV to VIII of the epithelial cycles. Light staining of PKB and p-PKB Ser^{473} was also detected at the sites between Sertoli cells and step 8 and 9 spermatids at stages VIII (Fig. 5, *D*, *L*, and *M*) and IX (Fig. 5, *E* and *N*). Moderate staining of immunoreactive PKB (Fig. 5, *F* and *G*) and p-PKB Ser^{473} (Fig. 5, *O* and *P*) was found between Sertoli cells and elongating spermatids at stages XII–III, consistent with their localization at the apical ES. Prominent PKB and p-PKB Ser^{473} staining was associated with the nuclei of Sertoli

F5 AQ: V AQ: W F4

balt3/zbc-bc/zbc-bc/zbc02805/zbc1105-05g saylora S=4 16/5/05 15:32 4/Color Figure(s) 4-7,10,11,13 ARTNO: M501049200

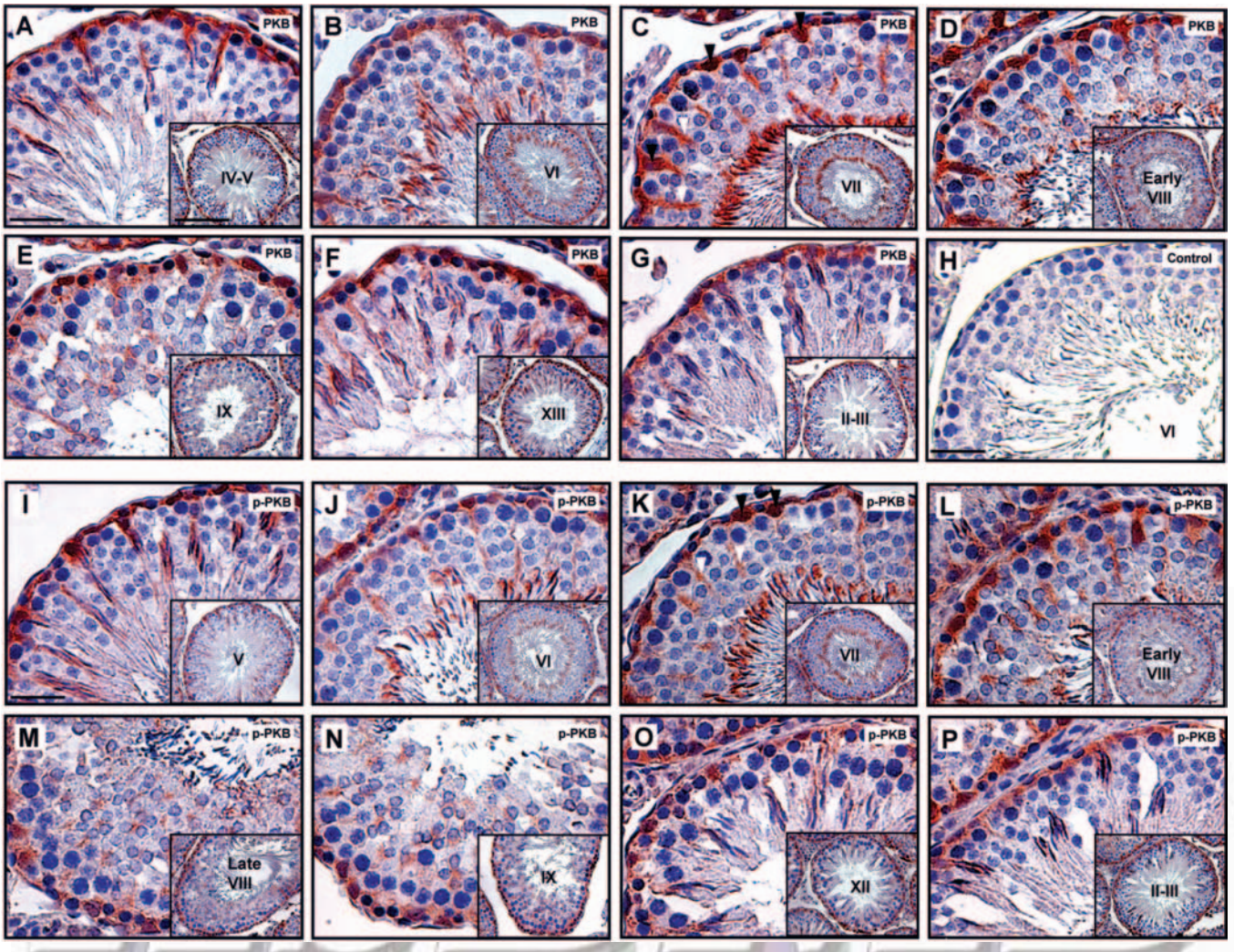

FIG. 5. **Micrographs of cross-sections of adult rat testes showing immunoreactive PKB (*A–H*) and p-PKB Ser^{473} (*I–P*) in the seminiferous epithelium at different stages of the epithelial cycle.** *A–G*, representative cross-sections of tubules at stages IV and V, VI, VII, early VIII, IX, XIII, and II and III, respectively, of the epithelial cycle; *I–P*, cross-sections of tubules at stages V, VI, VII, early VIII, late VIII, IX, XII, and II and III, respectively. Immunoreactive PKB and p-PKB Ser^{473} appear as reddish brown precipitates. The *insets* are selected regions of the seminiferous epithelium at lower magnification. *H*, corresponding control; sections were incubated with normal rabbit IgG replacing the primary antibody. *Scale bar* = 20 μm in *A*, which applies to *B–P*; *scale bar* = 100 μm in the *inset* in *A*, which applies to the *insets* in *B–P*.

cells (see *black arrowheads* in Fig. 5, *C* and *K*) at all stages of the epithelial cycle. The strong staining in the Sertoli cells was shown to extend toward the lumen, forming cytoplasmic ridges at stages VI–VIII (Fig. 5, *B-D* and *J–M*) and becoming very prominent at stage VII (see *white arrowheads* in Fig. 5, *C* and *K*). This was consistent with their localization at the basal and apical ES. In the basal compartment of the epithelium, immunoreactive PKB and p-PKB Ser^{473} were also found to associate with spermatogonia at all stages (Fig. 5).

Localization of PAK—The pattern of localization of PAK in the seminiferous epithelia of adult rat testes was similar to those of PI3K and PKB (Fig. 6 *versus* Figs. 4 and 5). PAK was localized to both apical and basal ES, largely around the heads of elongated spermatids at stages VI–VIII (Fig. 6, *A*, *B*, and *F*) and the perinuclear region of Sertoli cells at all stages. Moderate PAK staining was also found to associate with pachytene spermatocytes at stage VII (Fig. 6*A*) and stage VIII (Fig. 6*B*) and with Sertoli cell cytoplasmic ridges (Fig. 6, *A*, *B*, and *D*). Weak staining of PAK was associated with all stages of germ cells, including elongating spermatids at stages XII–V (Fig. 6, *C–E*), consistent with its localization at the ES site.

Co-localization of PI3K p85α and p-PKB Ser^{473} in the Seminiferous Epithelium

Because PI3K p85α (Fig. 4, *B* and *C*), PKB (Fig. 5, *B-D*), p-PKB Ser^{473} (Fig. 5, *J-M*), and PAK (Fig. 6, *A*, *B*, and *F*) were localized largely to the same sites at both the basal and apical ES, fluorescence microscopy was performed to assess the co-localization PI3K p85α and p-PKB Ser^{473} in the seminiferous epithelium. Merged images show that PI3K p85α and p-PKB Ser^{473} indeed were co-localized to both the basal and apical ES at stage V (Fig. 7, *C versus A* and *B*) and stage VI (Fig. 7, *F versus D* and *E*) of the epithelial cycle. The amount of immunoreactive PI3K p85α at the basal ES was reduced from stage V to VI (Fig. 7, *A versus D*), which is consistent with the immunohistochemistry data shown in Fig. 4*B*.

Analysis of Structural Interactions of PI3K p85α, PKB, and PAK with the ES-associated Protein Complexes and Cytoskeletal Proteins in Adult Rat Testes

To further elucidate the role of PI3K p85α, PKB, and PAK in ES dynamics, Co-IP was performed using lysates of seminiferous tubules isolated from 90-day-old rats (with negligible contamination of Leydig and myoid cells) with antibodies against

balt3/zbc-bc/zbc-bc/zbc02805/zbc1105-05g saylora S=4 16/5/05 15:32 4/Color Figure(s) 4-7,10,11,13 ARTNO: M501049200

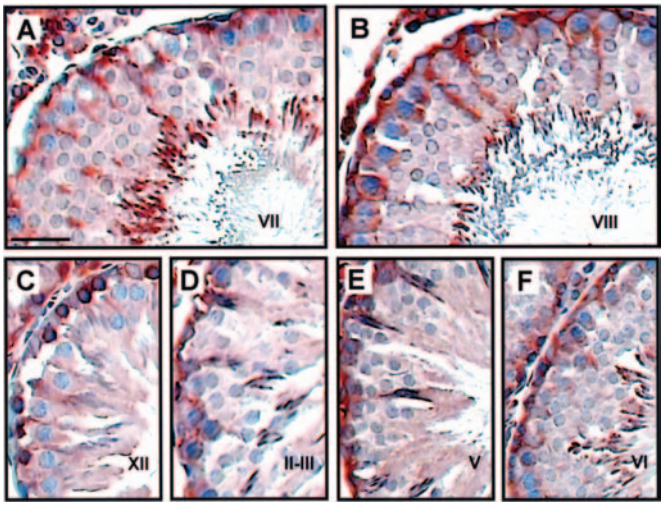

FIG. 6. **Micrographs of cross-sections of normal rat testes showing immunoreactive PAK in the seminiferous epithelium at different stages of the epithelial cycle.** *A–F*, representative cross-sections of seminiferous tubules at stages VII, VIII, XII, II and III, V, and VI, respectively, of the epithelial cycle. Immunoreactive PAK appears as a reddish brown precipitate. *Scale bar* = 20 μm in *A*, which applies to *B–F*.

F8 different ES-associated proteins. In Fig. 8*A*, 10 ES-associated proteins, including β1-integrin and its downstream signaling AQ: Y molecules and adaptors (FAK, p-FAK, PI3K, paxillin, p130^{Cas}, and vinculin), gelsolin, N-cadherin and nectin-3 were selected, and antibodies against these proteins were used for Co-IP. PI3K p85α was found to structurally associate with β1-integrin, FAK, p-FAK Tyr^{397}, paxillin, p130^{Cas}, vinculin, and gelsolin, but not with N-cadherin or nectin-3 (Fig. 8*A*). Interestingly, there was no structural association between PKB and any ES-associated proteins examined, including PI3K p85α (Fig. 8*A*). We next sought to investigate the structural interactions between PAK and proteins in the PI3K signaling pathway. Antibodies against FAK, p-FAK Tyr^{397}, c-Src, PI3K AQ: Z p85α, PDK1, PKB, and PTEN were used to pull down PAK. Only c-Src was structurally associated with both PAK1 (αPAK, 65 kDa) and PAK2 (γPAK, 62 kDa). PDK1 and PKB were structurally linked to PAK1, but not to FAK, p-FAK Tyr^{397}, PI3K p85α, or PTEN (Fig. 8*B*). Moreover, FAK, p-FAK Tyr^{397}, c-Src, PI3K p85α, PDK1, PKB, PAK, and PTEN were structurally associated with the two underlying cytoskeletal proteins actin and α-tubulin (Fig. 8*B*). c-Src, PDK1, PKB, and PTEN were also structurally linked to vimentin, another major cytoskeletal protein (Fig. 8*B*). Controls using seminiferous tubule lysates incubated with normal rabbit or mouse IgG for immunoprecipitation yielded no detectable band (data not shown).

Analysis of Changes in the Protein Levels of Different Protein Kinases and the Intrinsic Activity of PKB during AF-2364-induced Anchoring Junction Disruption in the Testis in Vivo

To induce progressive loss of germ cells from the seminiferous epithelium by disrupting anchoring junctions between Sertoli and germ cells in the testis, adult rats were fed a single dose of AF-2364 (50 mg/kg of body weight) by gavage. A transient induction of the protein levels of PI3K p85α, PI3K p110α, PDK1, and PTEN from 2 to 8 h, peaking at 2 h, was detected F9 (Fig. 9, *A* and *B*). The induced PI3K p85α, PI3K p110α, PDK1 (low M_r isoform), and PTEN levels decreased rapidly thereafter and became barely detectable by 15 days (Fig. 9*A*), whereas the protein level of higher M_r isoforms of PDK1 (Fig. 9*A*) remained steady until 15 days, but was increased by as much as 1.5-fold by 4 and 15 days (Fig. 9, *A* and *B*). Although the level of PKB remained relatively stable throughout the treatment period, a significant reduction was detected by 15 days post-treatment; a significant induction of p-PKB Thr^{308} and p-PKB Ser^{473} levels was detected from 4 h to 1 days. Thereafter, they returned to their basal levels at 2 days (Fig. 9, *A* and *B*). The induced p-PKB Thr^{308} and p-PKB Ser^{473} levels were also accompanied by a significant increase in intrinsic PKB kinase activity (Fig. 9, *C* and *D*). PAK, PAK1, and PAK2 was transiently stimulated as early as 2 h and persisted until 8 h; their levels were then reduced to their basal levels, but they became virtually not detectable by 4 days (Fig. 9, *A* and *B*). The changes in the protein level of ERK1/2 were similar to those of PKB. ERK1/2 remained at a relatively steady level throughout the treatment period until it decreased at 15 day (Fig. 9, *A* and *B*). One of its activated forms, p-ERK1 (Fig. 9, *A* and *B*), was increased by as much as 2.5-fold beginning at 8 h, remained high until 4 days, and then returned to its basal level at 15 days. Although the protein level of p-ERK2 in the adult rat testis was very low, a mild induction was detected at 4 days, followed by an ~8-fold stimulation at 15 days (Fig. 9, *A* and *B*). These changes in protein levels in the PI3K/PKB/ERK signaling pathway are the result of a disruption of Sertoli-germ cell anchoring junctions in the seminiferous epithelium because when rats were treated with a vehicle control (0.5% (w/v) methylcellulose with Milli-Q water), they failed to display any changes in these protein kinases when germ cells were not depleted from the epithelium (Fig. 9, *E versus A* and *B*).

Immunohistochemical Localization of PI3K p85α, PKB, and p-PKB Ser^{473} in the Seminiferous Epithelium of the Rat Testis during AF-2364-induced Anchoring Junction Disruption

Immunohistochemical localization of PI3K p85α, PKB, and p-PKB Ser^{473} in the seminiferous epithelium after AF-2364 treatment was performed using cross-sections of treated rats at selected time points. The AF-2364-induced increases in the protein levels of PI3K p85α and p-PKB Ser^{473} in the seminiferous epithelium were largely confined to the heads of elongating/elongated spermatids at 4 h, consistent with their localization at the apical ES (Fig. 10, *A*, *B*, *I*, and *J*). The F10 pattern of localization of PKB was also similar to that of its activated form (Fig. 10, *E* and *F versus I* and *J*). By 4 days and thereafter, most elongating/elongated and round spermatids were depleted from the tubule, and the number of spermatocytes was also significantly reduced by 15 days. Also, very weak staining of immunoreactive PI3K p85α and p-PKB Ser^{473} was detected in the seminiferous epithelium at this time (Fig. 10, *C* and *K*). Immunoreactive PKB was reduced in the epithelium at 4 (Fig. 10*G*) and 15 (Fig. 10*H*) days post-treatment. Immunoreactive PI3K p85α, PKB, and p-PKB Ser^{473} were not restricted to the basal ES site, but apparently also localized diffusely in the Sertoli cell cytoplasm at 4 days (Fig. 10, *C* and *D*, *G* and *H*, and *K* and *L*, respectively). These data are also consistent with the immunoblotting results shown in Fig. 9 (*A–E*).

Morphological Analysis and Kinetics of Elongating/elongated Spermatid Loss from the Seminiferous Epithelium of the Rat Testis during AF-2364-induced Anchoring Junction Disruption with and without Pretreatment with the PI3K-specific Inhibitor Wortmannin

To further elucidate the significance of PI3K in AF-2364-mediated anchoring junction disruption, wortmannin, a PI3K-

balt3/zbc-bc/zbc-bc/zbc02805/zbc1105-05g saylora S=4 16/5/05 15:32 4/Color Figure(s) 4-7,10,11,13 ARTNO: M501049200

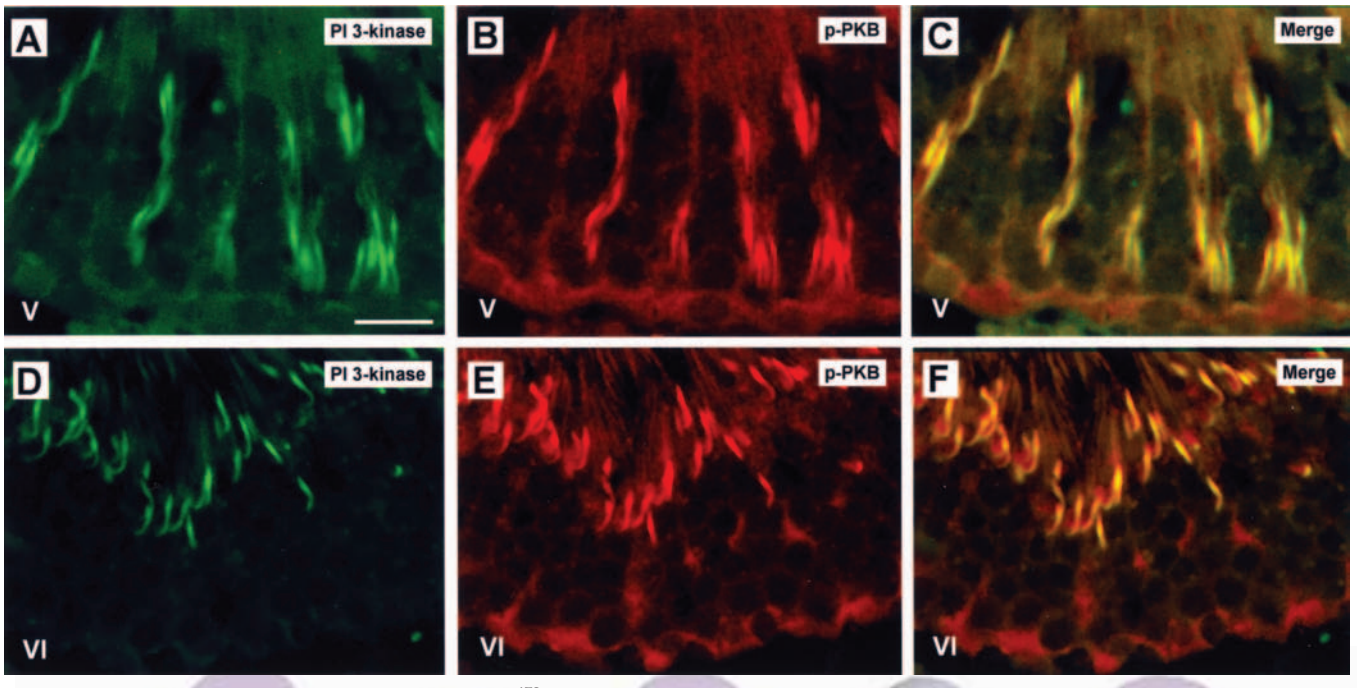

FIG. 7. **Co-localization of PI3K and p-PKB Ser^{473} in the seminiferous epithelium of adult rat testes by immunofluorescence microscopy.** *A* and *D*, immunofluorescent micrographs of cross-sections of adult rat testes showing the localization of immunoreactive PI3K in the epithelium at stages V and VI, respectively, of the epithelial cycle; *B* and *E*, immunofluorescent micrographs of the same sections showing the localization of immunoreactive p-PKB Ser^{473}; *C* and *F*, the corresponding merged images. *Scale bar* = 50 μm in *A*, which applies to *B–F*.

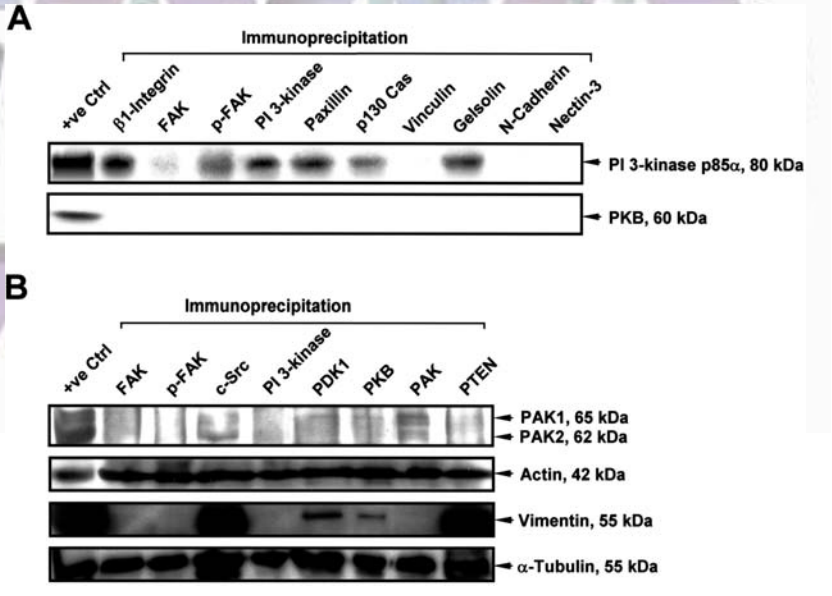

FIG. 8. **Association of ES-associated proteins with PI3K, PKB, PAK, actin, vimentin, and α-tubulin in the seminiferous epithelium of the rat testis as determined by Co-IP.** Lysates of seminiferous tubules with negligible Leydig and myoid cell contamination were used for Co-IP with antibodies against different ES-associated proteins. Immunocomplexes were subjected to immunoblotting and stained sequentially with anti-PI3K and anti-PKB antibodies (*A*) or anti-PAK, anti-actin, anti-vimentin, and anti-α-tubulin antibodies (*B*). *ve control*, vehicle control.

AQ: AA

specific inhibitor, was used to determine whether it could delay the kinetics of germ cell loss. When rats were pretreated with 0.5 mM wortmannin via intratesticular injection, a significant delay in the loss of elongating/elongated spermatids from the seminiferous epithelium was observed at 2 and 4 days after AF-2364 treatment (Fig. 11, *D–F versus A–C* and *J*). However, inhibitor pretreatment had no effect on the delay of the AF-2364-induced loss of elongating/elongated spermatids from the epithelium at 6 days compared with AF-2364 treatment alone (Fig. 11, *F versus C* and *J*), whereas the loss of spermatocytes was clearly deferred by the inhibitor pretreatment (Fig. 11, *F versus C*). Pretreatment of the testes with wortmannin alone at this dose for up to 6 days had no effect on the germ cell population in the epithelium (Fig. 11, *G–I*).

F11

AQ: BB

Changes in the Protein Levels of PKB, p-PKB Thr^{308}, PDK1, PAK, ERK, and p-ERK during AF-2364-induced Germ Cell Loss from the Epithelium with and without Wortmannin Pretreatment

When wortmannin was administered to rat testes prior to AF-2364 treatment and the testes were removed 2 days thereafter, wortmannin not only blocked the AF-2364-mediated induction of p-PKB Thr^{308}, but it also triggered the loss of PAK2 (not PAK1) from the seminiferous epithelium (Fig. 12). At the same time, PTEN was induced by wortmannin pretreatment (Fig. 12). However, induction of p-ERK1/2 mediated by AF-2364 treatment was further up-regulated after wortmannin pretreatment, yet wortmannin failed to affect the levels of PDK1, PKB, and ERK during ES disruption (Fig. 12).

F12

balt3/zbc-bc/zbc02805/zbc1105-05g saylora S=4 16/5/05 15:32 4/Color Figure(s) 4-7,10,11,13 ARTNO: M501049200

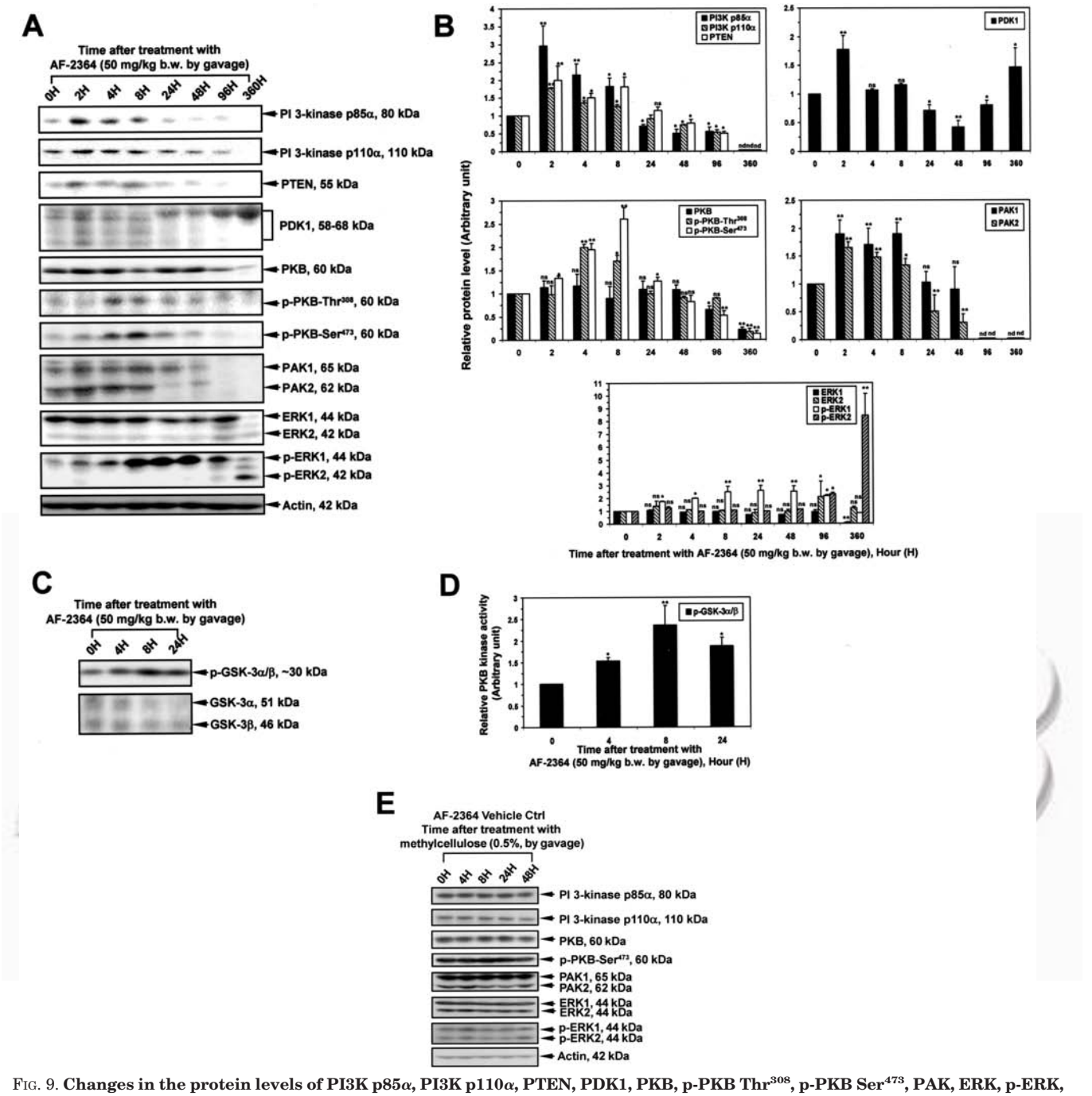

FIG. 9. **Changes in the protein levels of PI3K p85*α*, PI3K p110*α*, PTEN, PDK1, PKB, p-PKB Thr^{308}, p-PKB Ser^{473}, PAK, ERK, p-ERK, and phospholipase Cγ and the intrinsic kinase activity of PKB during AF-2364-induced germ cell loss from the seminiferous epithelium of the rat testis *versus* control rats receiving vehicle (0.5% methylcellulose) alone.** *A–D*, adult rats (~300 g of body weight) were treated with AF-2364 at 50 mg/kg of body weight (*b.w.*) by gavage at time 0 with $n = 3$ per time point. Rats at time 0 served as controls. *E*, another group of controls (*Ctrl*), which received 0.5% (w/v) methylcellulose with Milli-Q water alone, was also included. Testes were removed from animals at the specified time points. *A*, equal amounts of testis lysates (~100 μg of protein/lane) were resolved by SDS-PAGE (7.5 or 12.5% T) under reducing conditions and subjected to immunoblot analysis using the primary antibodies as indicated. *C*, ~200 μg of testis lysates from AF-2364-treated rats was prepared and immunoprecipitated using immobilized anti-PKB antibody. Immunocomplexes were incubated in kinase buffer containing the GSK-3 fusion protein (a putative PKB substrate) and ATP. GSK-3 phosphorylation was analyzed using anti-p-GSK antibody (*upper panel*). Total GSK-3α and GSK-3β levels are shown (*lower panel*). *B* and *D*, shown are the histograms for the corresponding data in *A* and *C*, respectively, following densitometric scanning of immunoblots with n = three different rats for each time point. The results were normalized against the protein level at time 0, which was arbitrarily set at 1. Each *bar* represents the mean ± S.D. of three experiments. Each experiment had replicate cultures. *, $p < 0.05$, significantly different by analysis of variance; **, $p < 0.01$; *ns*, not significantly different; *nd*, not detectable.

AQ: PP

Changes in the Kinetics of Spermatid Loss from the Epithelium by Blocking β1-Integrin Function Using Specific Antibodies

To further delineate the significance of the α6β1-integrin·laminin γ3 protein complex (which also serves as the crucial upstream signaling protein complex) in regulating Sertoli-germ cell adhesion function in the epithelium, testes were administered anti-β1-integrin IgG (50 μg/testis *versus* rabbit IgG) prior to AF-2364 treatment (Fig. 13). When β1-integrin function was blocked by the specific antibody, AF-2364-induced spermatid loss from the seminiferous epithelium was significantly delayed by day 6, which was not seen when rat testes received IgG alone (Fig. 13, *E versus H* and *A*, *B*, *D*, and *G*).

F13

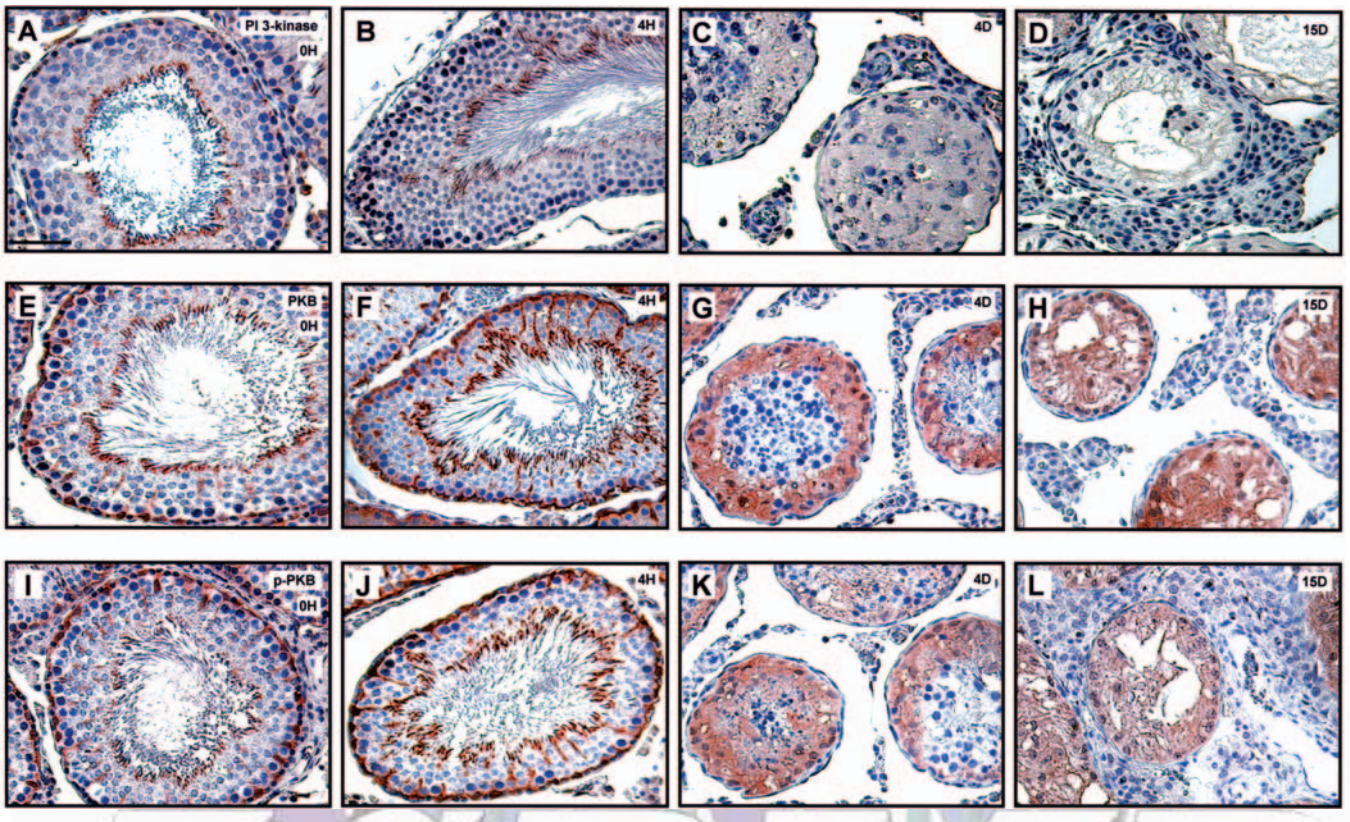

FIG. 10. **Changes in the localization patterns of PI3K, PKB, and p-PKB in the seminiferous epithelium of the rat testis during AF-2364-induced anchoring junction disruption as determined by morphological analysis.** *A–D*, representative micrographs illustrating the localization pattern of PI3K (reddish brown precipitate) in the seminiferous epithelia from normal rat testes at 0 h, 4 h, 4 days, and 15 days, respectively, after AF-2364 treatment (one dose of 50 mg/kg of body weight by gavage); *E–H* and *I–L*, corresponding micrographs from the same groups of animals following AF-2364 treatment as those in *A–D*, but immunostained for PKB and p-PKB, respectively. These micrographs are representative of results from three different experiments. *Scale bar* = 40 μm in *A*, which applies to *B–L*.

AQ: QQ

Although testes that were pretreated with anti-β1-integrin IgG also displayed clear signs of germ cell loss from the epithelium by day 12 (Fig. 13, *F versus C*), *e.g.* the tubule lumen was filled with departing germ cells, the blockade of β1-integrin function had significantly delayed the kinetics of germ cell loss (Fig. 13, *C*, *F*, and *I*).

DISCUSSION

ES Is a Hybrid Cell-Matrix-Cell AJ Type That Utilizes FA Components to Facilitate Germ Cell Movement

The translocation of developing germ cells across the seminiferous epithelium during the epithelial cycle is an essential cellular phenomenon of spermatogenesis. This process requires extensive junction restructuring at the cell-cell interface involving tight and anchoring junctions (for reviews, see Refs. 1, 6, and 7). The mechanism(s) that regulates this event is virtually unknown. This is due to the lack of suitable *in vitro* and *in vivo* study models. Herein, we have reported the results of studies utilizing two models to identify the signaling pathway that regulates anchoring junction restructuring in the seminiferous epithelium of the rat testis. The apical ES is composed of FA complex-associated proteins usually restricted to the cell-matrix interface in other epithelia, including β1-integrin, vinculin, c-Src, C-terminal Src kinase, integrin-linked kinase, PI-4,5-P_2, phospholipase Cγ, Fyn, and Keap1 (for reviews, see Refs. 1, 2, and 7). More important, phosphorylated FAK (the activated form of FAK) was shown to be a potential linker of β1-integrin at the apical ES, recruiting peripheral proteins to the apical ES during its remodeling (8). These results, coupled with recent findings that laminin γ3 (a novel non-basement membrane extracellular membrane protein residing in spermatids) is the putative binding partner for β1-integrin in Sertoli cells and the presence of proteases (*e.g.* MMP-2 and membrane type-1 MMP) and protease inhibitors (*e.g.* TIMP-2) that likely regulate the β1-integrin·laminin γ3 complex at the ES site (38), have provided an entirely new concept on apical ES regulation. For instance, the ES is being regarded as a *cell-matrix-cell* junction AJ type with the properties of both cell-cell actin-based AJs and cell-matrix FAs to facilitate germ cell movement in the epithelium. It is plausible that the events of germ cell movement at the ES interface share the features of FA remodeling during cell-matrix restructuring (7, 55). In this study, we have identified the signal transducers downstream of β1-integrin and FAK at the apical ES, including PI3K (a lipid kinase) and p-PKB and PAK2 (protein kinases), which in turn activate p-ERK. The net result of such activation likely affects the actin cytoskeleton. Interestingly, these lipid and protein kinases are also restricted to the cell-matrix anchoring junction site (*viz.* the FA complex) in other epithelia, yet they are found in the apical ES, as reported herein. Perhaps the most important of all, by blocking the function of α6β1-integrin with anti-β1-integrin antibody, we have shown that this can indeed delay AF-2364-induced germ cell loss from the epithelium. These findings have unequivocally demonstrated the significance of the integrin·laminin complex at the ES site, which serves as the initial signal transducer in the regulation of Sertoli-germ cell adhesion function in the seminiferous epithelium. These findings also strengthen the notion that the apical ES is indeed a hybrid cell-cell and cell-matrix actin-based anchoring junction type utilizing pro-

AQ: CC

balt3/zbc-bc/zbc-bc/zbc02805/zbc1105-05g saylora S=4 16/5/05 15:32 4/Color Figure(s) 4-7,10,11,13 ARTNO: M501049200

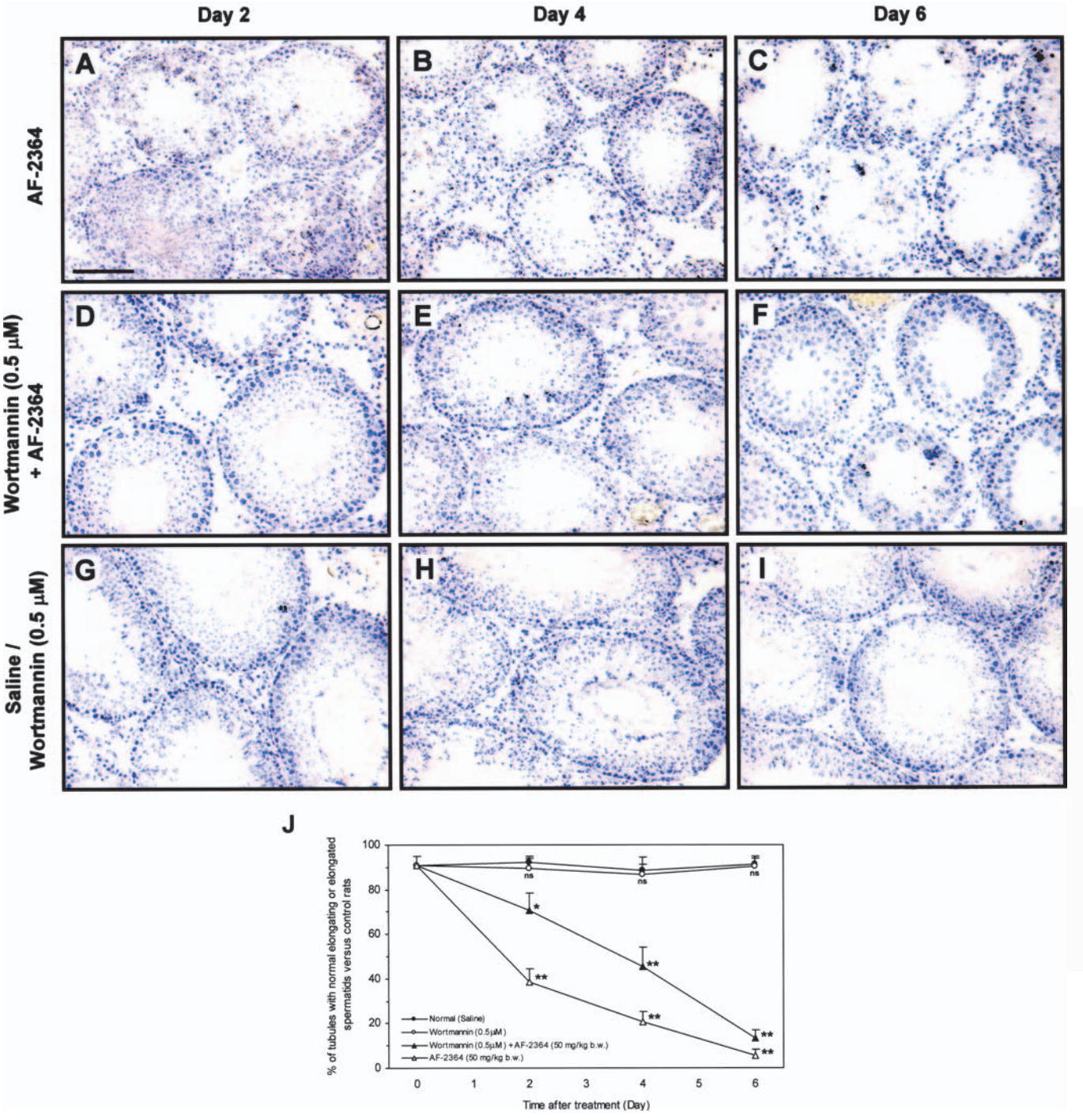

FIG. 11. **Kinetics of the loss of elongating/elongated spermatids from the seminiferous epithelium after treatment of rats with AF-2364 or wortmannin + AF-2364 *versus* controls or wortmannin alone as determined by morphological analysis.** Shown are cross-sections of adult rat testes, where, at time 0, rats had received AF-2364 alone (50 mg/kg of body weight (*b.w.*) by gavage) (*A–C*), 0.5 μM wortmannin (via intratesticular administration) and AF-2364 (50 mg/kg of body weight by gavage) (*D–F*), saline alone (intratesticular administration) (*G*), or 0.5 μM wortmannin alone (intratesticular administration) (*H* and *I*), followed by termination ($n = 3$ per time point in each treatment group) at different time points. The composite results illustrating the kinetics of elongating/elongated spermatid loss from the seminiferous epithelium are shown by plotting changes in the percentage of tubules having elongating/elongated spermatid loss from the epithelium after different treatments *versus* controls (no treatment) against time (in days) after treatment (*J*). For statistical analysis, each treatment group was compared with the control group at the corresponding time using Student's *t* test. *, $p < 0.05$, significantly different; **, $p < 0.01$, significantly different; *ns*, not significantly different. *Scale bar* = 120 μm in *A*, which applies to *B–I*.

teins that are usually restricted to the cell-matrix interface to regulate its dynamic restructuring pertinent to spermatogenesis. Furthermore, the β1-integrin/p-FAK/PI3K/p-PKB/PAK2/ERK signaling pathway is used to regulate Sertoli-germ cell anchoring junction dynamics both *in vitro* and *in vivo*, in particular at the apical ES.

Lipid and Protein Kinases Are Crucial to Sertoli-Germ Cell AJ Assembly Such as the ES

Role of PI3K—The synthesis and breakdown of PPIs by the interplay of lipid kinases (*e.g.* PI3K) and PPI phosphatases (*e.g.* myotubularins and MTM proteins) are important to many cel-

AQ: DD

balt3/zbc-bc/zbc-bc/zbc02805/zbc1105-05g saylora S=4 16/5/05 15:32 **4/Color Figure(s) 4-7,10,11,13** ARTNO: M501049200

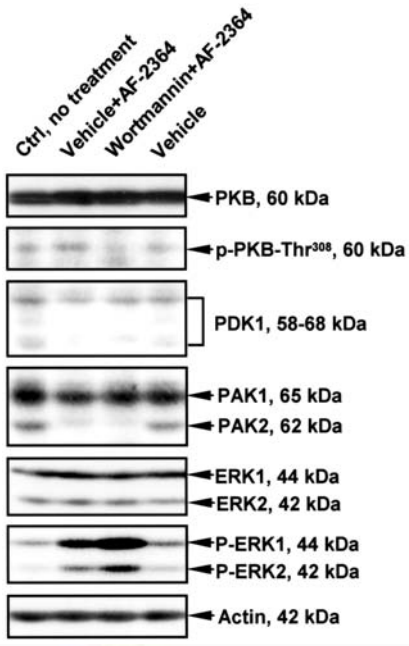

FIG. 12. **Changes in target proteins in the ERK signaling pathway during AF-2364-induced germ cell loss from the seminiferous epithelium with and without pretreatment with wortmannin.** Immunoblotting was performed using testis lysates (~100 μg of total protein from each sample/lane) obtained from rats treated with AF-2364 alone (*Vehicle + AF-2364*) and after pretreatment with wortmannin + AF-2364 *versus* controls (*Ctrl*; vehicle alone and normal testes without any treatment) (see "Experimental Procedures"). Blots were immunostained using specific antibodies against PKB, p-PKB, PDK1, PAK, ERK, and p-ERK. The same blot was also reprobed with anti-actin antibody to assess equal protein loading. Results are from three different experiments using different lysate samples from different rats and represent the composite results of these analyses.

lular processes. For example, PPI can regulate the rearrangement of the actin cytoskeleton, which in turn affects cell adhesion and migration (56–58). Also, PI3K regulates F-actin polymerization (for review, see Ref. 12). In this study, when Sertoli-germ cells were co-cultured for 2 days, functional ES structures and desmosome-like junctions were established at the cell-cell interface, yet at the time germ cells were attaching to Sertoli cells before these anchoring junctions were established (*i.e.* between 1 h and 1 days) (32), a significant induction of both the regulatory p85α and catalytic p110α subunits of PI3K was detected. These data seemingly suggest that phosphorylation of PPI at the D3 position is involved in Sertoli-germ cell AJ assembly. This view is further supported by the localization of immunoreactive PI3K p85α at the site of ES in the epithelium as reported herein and the presence of PI-4,5-P_2 in the ES as reported previously (20). These observations thus suggest that PI3K p85α is directed to the site during ES assembly; it also recruits the catalytic p110α subunit, phosphorylating PI-4,5-P_2 and leading to actin polymerization at the site of ES.

Role of PI-3,4,5-P_3, PKB, PDK1, PAK2, and ERK—PI3K-generated PI-3,4,5-P_3 can lead to the PH domain-dependent recruitment of PKB to the plasma membrane, where PKB is subsequently activated by PDK1 and an unidentified Ser^{473} kinase, which phosphorylate Thr^{308} and Ser^{473}, respectively. PDK1 is also a Ser/Thr protein kinase and binds to PPI and co-localizes with PKB at the cell membrane. The activated PKB can in turn induce its downstream effector (PAK). This signaling pathway plays a crucial role in actin reorganization and confers FA-mediated cell migration through the activation of ERK (14, 16). We have reported herein that PDK1, p-PKB Thr^{308}, p-PKB Ser^{473}, PAK2, and p-ERK (but not their inactive non-phosphorylated forms) were induced during Sertoli-germ cell AJ assembly. More important, these changes were shown to be associated with an increase in intrinsic PKB kinase activity. These results, coupled with immunohistochemical data illustrating that PKB, p-PKB Ser^{473}, and PAK were all localized to the ES site, have thus raised the possibility that PKB, PAK, and ERK are the downstream signal transducers of the PI3K pathway during ES assembly. The Co-IP studies presented herein have also supported their likely involvement in actin reorganization at the ES site because PI3K p85α, PDK1, PKB, PAK, and ERK are structurally associated with actin (data not shown). Numerous attempts were made to localize PDK1 in the seminiferous epithelium of the rat testis; however, its antibody failed to yield satisfactory results. As such, PDK1-mediated PKB phosphorylation at the ES site remains to be characterized in future studies. Nonetheless, there is accumulating evidence that the PI3K/PKB pathway plays an important role in AJ dynamics via its effects on F-actin recruitment to the cell-cell contact site (18, 19). For instance, the activation of PI3K can recruit Tiam-1, a GTP exchange factor, to AJs in Madin-Darby canine kidney cells, resulting in the activation of Rac GTPases (59). In studies using keratinocytes, Rac GTPase was shown to play a crucial role in forming and stabilizing AJs by recruiting F-actin to these junctions (60, 61). Collectively, these findings imply the role of PI3K in AJ and actin dynamics. Furthermore, this model was supported by studies using inhibitors (*e.g.* LY294002); for example, inhibition of PI3K can destabilize AJs in mammary epithelial cells (62), and such inhibition can also perturb AJ integrity in Caco-2/15 cells by reducing the levels of cytoskeleton-associated E-cadherin and β-catenin (19). The data presented herein further strengthen the notion that the PI3K/PKB/PAK/ERK signaling pathway is crucial to AJ dynamics via actin reorganization, including the ES site.

Role of PAK1—PAKs belong to a family of conserved Ser/Thr protein kinases, with six members known to date: PAK1–6 (for reviews, see Refs. 24 and 25). All PAKs contain an N-terminal regulatory domain and a C-terminal kinase domain. The PAK family can be classified into two subgroups: Group 1, consisting of PAK1 (also referred to as αPak), PAK2 (γPak), and PAK3 (βPak), which share >90% homology in their kinase domain and 73% overall homology in their entire sequence; and Group 2, consisting of PAK4–6, which share only ~50% homology with the PAK1 kinase domain (for reviews, see Refs. 24 and 25). Because PAK1 can be phosphorylated by PKB at Ser^{21}, leading to the stimulation of PAK1 activity in a GTPase-independent manner (26), Group 1 PAKs were thus selected to be examined in this study using anti-PAK1 antibody that can cross-react with PAK1–3. Co-IP using anti-PKB antibody showed that it can pull down the PKB·PAK1 complex from tubule lysates, confirming the possibility that PAK1 is a PKB effector in the testis. Previous studies have shown that, in addition to PKB, PAK1 is also a substrate of PDK1, which can phosphorylate PAK primarily at Thr^{423} residue and promote the activation of NIH-3T3 cells (52). This effect of PDK1 on PAK activation appears to be sphingosine-dependent and may be independent of 3-phosphoinositides because it cannot be blocked by wortmannin (63). The fact that PDK1 can form a protein complex with PAK1 in lysates of seminiferous tubules implies that PAK1 is a likely substrate of PDK1 in the testis. Although the protein level of PAK1 was not induced at the time germ cells attached to Sertoli cells *in vitro*, work is now in progress to determine whether PAK1 can be phosphorylated during Sertoli-germ cell AJ assembly. It is of interest to note that c-Src was shown to associate with PAK-1 and PAK-2 by Co-IP and as reported herein and that c-Src was

AQ: EE

balt3/zbc-bc/zbc02805/zbc1105-05g saylora S=4 16/5/05 15:32 4/Color Figure(s) 4-7,10,11,13 ARTNO: M501049200

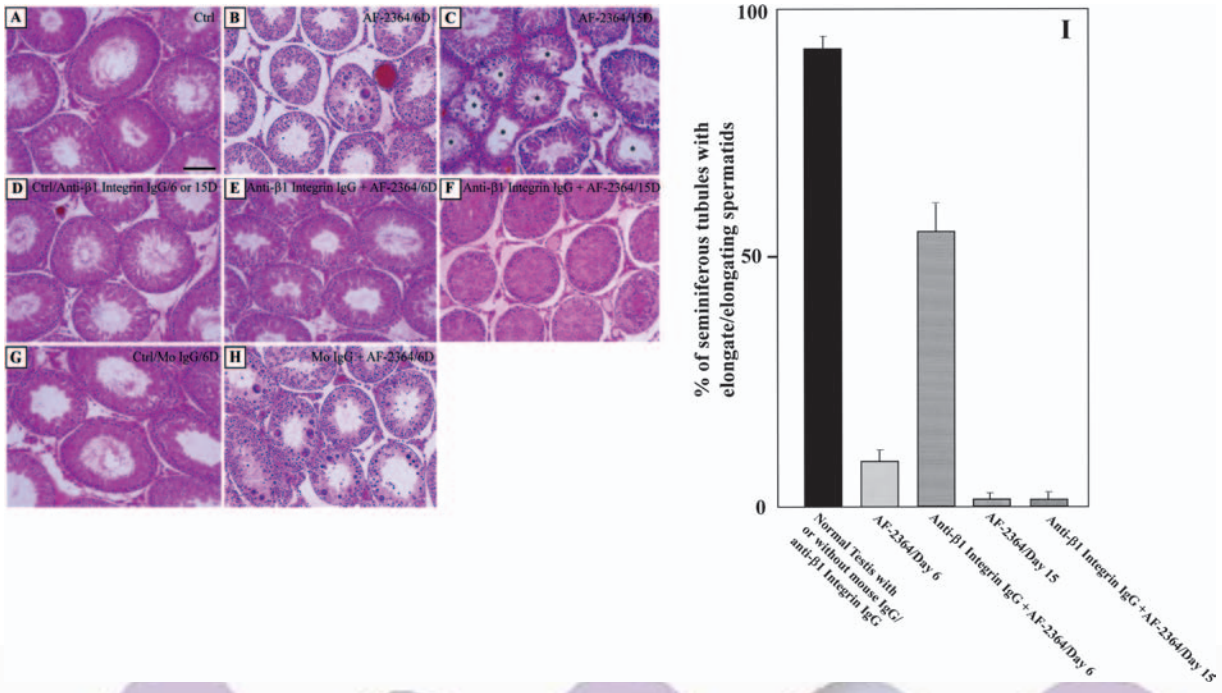

FIG. 13. **Effects of AF-2364-induced germ cell loss from the seminiferous epithelium following blocking β1-integrin function using a specific monoclonal antibody.** Adult rats (~300 g of body weight, $n = 3$ for each time point in each treatment group) received no treatment (*A*; control (*Ctrl*)), anti-β1-integrin IgG (50 μg/testis) (*D–F*), or normal mouse (*Mo*) IgG (*G* and *H*) via intratesticular injection in the left testis (two sites, ~100 μl/site) using a 27-gauge needle. The right testis, which served as the corresponding control, received either no treatment or PBS (*B* and *C*). Rats were then treated with (*B*, *C*, *E*, *F*, and *H*) or without (*A*, *D*, and G) a single dose of AF-2364 (50 mg/kg of body weight) by gavage to induce germ cell loss from the epithelium, and animals were killed on days 6 (*6D*) and 15 (*15D*) to assess seminiferous epithelial damage as described under "Experimental Procedures" using paraffin sections stained with hematoxylin and eosin. *Scale bar* = 120 μm in *A*, which applies to *B–H*. The bar graph shows the percentage of tubules containing elongating/elongated spermatids in the epithelium after different treatments (*I*). About 100 tubules from each testis were examined and scored (tubules with no elongating/elongated spermatids in the epithelium were scored as damaged tubules), and at least three testes from different rats were scored. *rbIgG*, rabbit IgG.

AQ: RR

localized to the apical ES (64). These results thus suggest the involvement of c-Src in PAK function at the ES site. A previous study has shown that coexpression of Src family tyrosine kinases and PAK2 can induce the activation of GTPases (*e.g.* Rac1 and Cdc42) possibly via phosphorylation of PAK2 at Tyr^{130} (65). As such, c-Src may mediate the activity of PAK2 via phosphorylation. This possibility must be validated in future studies.

Role of PTEN—PTEN is a major lipid phosphatase in multiple epithelial cells that catalyzes dephosphorylation of PI-3,4,5-P_3 and PI-3,4-P_2 at the D3 position, thus reducing the pool of lipids capable of binding to PH domain-dependent protein kinases (16). In Sertoli-germ cell co-cultures, the protein level of PTEN remained relatively steady when PI3K p110α was significantly induced at the time germ cells adhered to Sertoli cells *in vitro*, further illustrating the involvement of PI-3,4,5-P_3 and its downstream PH domain-dependent effectors in Sertoli-germ cell AJ assembly. In chemotaxing cells, PI3K and PTEN exhibit reciprocal patterns of spatial localization (for review, see Ref. 12). Interestingly, the localizations of PI3K p85α and PTEN in the seminiferous epithelium of the rat testis also display such reciprocal patterns. For instance, immunoreactive PI3K p85α was predominantly localized at the apical ES, surrounding the heads of elongating/elongated spermatids from stages IV to VIII. However, greatly diminished levels of immunoreactive PI3K p85α were accompanied by an increase in the localization of PTEN at the apical ES site just before spermiation, between late stage VIII and early stage IX of the epithelial cycle. This observation suggests that the negative regulation of PI3K-mediated lipid phosphorylation by PTEN is needed, perhaps necessary, for spermiation. Although the precise mechanism(s) by which PI3K and PTEN are utilized in spermiation remains to be explored, an alteration of F-actin polymerization at the apical ES site may be one of the downstream effects because a detailed analysis of PI3K and PTEN mutants suggests that the PI3K pathway regulates F-actin assembly (for review, see Ref. 12).

Role of Phospholipase Cγ—In this study, the protein level of phospholipase Cγ, a phosphoinositide-specific phospholipase that can hydrolyze PI-4,5-P_2, resulting in the release of gelsolin (an actin-severing protein) and the subsequent loss of actin from the ES site (20), was shown to decrease gradually during Sertoli-germ cell AJ assembly *in vitro*. This thus implicates actin polymerization as a vital process in Sertoli-germ cell apical ES dynamics. Fig. 13 also summarizes the possible involvement of these kinases in the signaling pathway that regulates Sertoli-spermatid adhesion function at the apical ES site.

PI3K in Basal ES and TJ Dynamics at the BTB

The results of immunohistochemistry studies shown herein demonstrated the presence of PI3K p85α, PKB, and PAK in the basal compartment of the seminiferous epithelium at the BTB site, suggesting their involvement in basal ES and BTB dynamics; however, the mechanism(s) is virtually unknown. The participation of PI3K/PKB in TJ dynamics is not unprecedented. For instance, the vascular permeability factor can significantly enhance the permeability of aortic endothelial cells via a putative signaling pathway sequentially involving c-Src, ERK, JNK, and PI3K/PKB. This leads to redistribution of actin and several TJ proteins (*e.g.* ZO-1 and occludin) and loss of the endothelial cell TJ barrier function (66).

balt3/zbc-bc/zbc02805/zbc1105-05g saylora S=4 16/5/05 15:32 4/Color Figure(s) 4-7,10,11,13 ARTNO: M501049200

p-FAK Tyr^{397} Is the Potential Upstream Protein Kinase That Mediates Membrane Localization of PI3K p85α at the Apical ES, Forming the PI3K·p-FAK Regulatory Protein Complex

Class I PI3Ks are largely cytosolic in resting cells, but upon stimulation, they are recruited to membranes via interactions with receptors or adaptors (for review, see Ref. 13). As such, it is of interest to identify the receptor(s) and/or adaptor(s) that directs PI3K to the ES site. Co-IP studies have shown that activated FAK (p-FAK-Tyr^{397}) is the potential receptor that triggers the membrane recruitment of the PI3K p85α adaptor subunit in the seminiferous epithelium. Previous studies have shown that p-FAK Tyr^{397} is a crucial linker for β1-integrin to recruit other regulatory components to the apical ES site (7, 8); the additional data presented herein have thus raised the possibility that PI3K p85α is also one of the SH2 domain-containing ES proteins recruited by activated FAK for its membrane localization at the apical ES site. In addition to FAK, PI3K p85α was also found to interact with other ES proteins, including β1-integrin, paxillin, p130^{Cas}, vinculin, and gelsolin, but not N-cadherin or nectin-3. These results thus suggest that PI3K is involved in β1-integrin-mediated (but not cadherin- or nectin-3-mediated) ES dynamics. In this context, it is of interest to note that none of the ES proteins examined herein by Co-IP was structurally associated with PKB. This may be due to the fact that, although PKB is a PI3K effector, its activation process involves intermediate PI3K-generated PI-3,4,5-P_3, which acts as a membrane anchor that provides the PH domain-binding site for PKB. As such, PKB does not form a stable protein complex with PI3K p85α in the seminiferous epithelium, yet in fluorescence microscopy studies, PI3K p85α co-localized with PKB (data not shown) and p-PKB Ser^{473} to both the basal and apical ES, supporting the notion that PKB lies downstream of PI3K functionally at the ES site.

AQ: FF

Functional Significance of Lipid and Protein Kinases in Cytoskeletal Dynamics

Actin microfilaments, intermediate filaments, and microtubules are the three cytoskeletons in the testis. The ES is a testis-specific AJ structure utilizing actin as the attachment site. The association of FAK, p-FAK Tyr^{397}, c-Src, PI3K p85α, PDK1, PKB, PAK, and PTEN with actin as demonstrated by Co-IP studies further supports that such a signaling pathway acts on ES dynamics through actin reorganization. In addition to their association with actin, they were also shown to associate with α-tubulin (a subunit of the microtubule), suggesting their likely participation in microtubule reorganization in the seminiferous epithelium, albeit the precise mechanism(s) is not yet known. Indeed, recent evidence has implicated PAKs in microtubule reorganization (67). For instance, PAK1 phosphorylates stathmin at Ser^{16}, stabilizing microtubules (68). In general, microtubules have well defined roles in Sertoli cells (for review, see Ref. 3) and are found at the site of ES (69). They are known to maintain Sertoli cell shape, to orient spermatids in the epithelium and their translocation, and to adjust the contour of the Sertoli cell membrane to adapt the irregularly shaped spermatid heads that are lodged within crypts during spermatogenesis. As such, it is not entirely unexpected that the most striking changes in microtubule organization occur during spermiogenesis (for review, see Ref. 3). For the intermediate filament network that is the attachment site of the desmosome-like junction, only c-Src, PTEN, PDK1, and PKB were found to structurally associate with vimentin (a structural component of the intermediate filament). Recent findings have suggested that PAKs may have a crucial role in intermediate filament reorganization. For instance, PAK1 phosphorylates

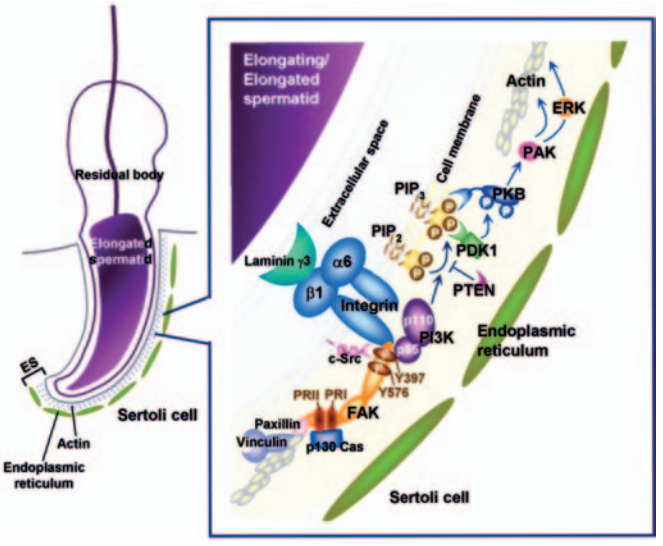

FIG. 14. **Schematic drawing illustrating the plausible cascade of events involving the α6β1-integrin·laminin γ3 protein complex and the downstream signaling molecules that regulate apical ES dynamics in the seminiferous epithelium of the rat testis.** As reported herein, it is likely that AF-2364-induced spermatid loss from the epithelium involves an initial activation of β1-integrin, which in turn transmits the signal downstream involving PI3K, PTEN, PDK, PKB, PAK, and ERK. The net result of this interaction changes the association of the α6β1-integrin·laminin γ3 protein complex with its downstream signaling molecules, adaptors, and the actin-based cytoskeletal network at the apical ES site, affecting Sertoli-germ cell adhesion in the epithelium. This is likely one of the regulatory signaling pathways that regulate Sertoli-germ cell adhesion in the seminiferous epithelium during the epithelial cycle pertinent to spermatogenesis. *PIP_2*, phosphatidylinositol 4,5-bisphosphate; *PIP_2*, phosphatidylinositol 3,4,5-trisphosphate.

AQ: SS

desmin and inhibits its ability to bind to the intermediate filament (70). PAK1 also regulates the reorganization of vimentin filaments through direct vimentin phosphorylation (71). Although PAK was not shown to associate with vimentin in the seminiferous epithelium, it is of interest to define the role(s) of c-Src, PTEN, PDK1, and PKB and their mechanism(s) in intermediate filament reorganization in the testis. Collectively, we postulate that the PI3K·PKB·PAK·ERK protein complex, plausibly working in concert with PTEN/PDK1, lies downstream of β1-integrin/p-FAK and is crucial in regulating ES dynamics via its effects on the cytoskeletal network (Fig. 14).

F14

AF-2364-induced Germ Cell Loss Is Regulated, at Least in Part, Via the β1-Integrin/PI3K/PDK1/p-PKB/PAK/p-ERK Signaling Pathway

AF-2364 induces germ cell loss from the seminiferous epithelium, which apparently exerts its effects initially at the apical ES (48, 49). Interesting, this event also induces the activation of several signal transducers in the PI3K pathway. For instance, a transient induction of the protein levels of PI3K p85α, PI3K p110α, PTEN, and PDK1 was first detected at ~2 h post-treatment, followed by induction of p-PKB Thr^{308}, p-PKB Ser^{473} and its intrinsic kinase activity, PAK2, and PAK1, which were induced by 4–8 h. p-ERK1 was the last protein to be induced (by ~8 h). This time course coincides with the time of depletion of elongating/elongated spermatids from the epithelium, followed by round spermatids, suggesting that such an activation of the PI3K pathway plays a crucial role in AF-2364-mediated ES disruption. In this context, it is of interest to note that the potential upstream mediators of PI3K, (*viz.* β1-integrin and p-FAK Tyr^{397}) were previously shown to be induced by ~1 h post-treatment (8), prior to PI3K induction, suggesting that the PI3K pathway lies downstream of β1-

integrin/p-FAK Tyr^{397} in the AF-2364-induced ES disassembly. Similar to β1-integrin and p-FAK (8), a potential bifunctional role of PI3K signaling in regulating both junction disassembly and assembly was also observed, albeit the precise mechanism remains obscure. The finding that wortmannin, a specific inhibitor of PI3K, can indeed block the AF-2364-mediated induction of p-PKB Thr^{308} and PAK2, delaying the loss of elongating/elongated spermatids from the epithelium, unequivocally illustrates the significance of the PI3K/PKB/PAK2 signaling pathway in ES dynamics. It also demonstrates that the AF-2364-mediated induction of PKB and PAK2 is a PI3K-dependent event. Although PDK1 and PAK1 were not affected by wortmannin pretreatment, it is plausible that their phosphorylated status (but not their total protein levels) were affected. This possibility must be investigated in future studies. Nonetheless, these findings, coupled with the fact that blocking β1-integrin using a specific antibody can significantly delay AF-2364-induced germ cell (in particular, elongating/elongated spermatids) loss from the seminiferous epithelium, unequivocally demonstrate that one of the putative upstream signal transducers of the PI3K/PKB/PAK2 signaling pathway is β1-integrin (Fig. 14).

Role of PKB, PAK, and ERK in Actin-mediated Junction Dynamics and during AF-2364-induced Germ Cell Loss from the Seminiferous Epithelium

PKB, PAK, and ERK are known regulators of actin dynamics (for reviews, see Refs. 17, 24, and 72). For instance, PKB can be targeted to the actin cytoskeleton, which is mediated by small GTPases such as Cdc42 (73). PAK1 is also localized to FAs at the cell-matrix interface, conferring cell migration (74). For instance, activated PAK1 takes part in the formation of vinculin-containing focal complexes at the leading edge of migrating cells (75). Activated PAK1 can also induce the loss of actin stress fibers and increase FA turnover at the rear end of a migrating cell (75). Although the details of the changes mediated by PAK1 are not entirely understood, they involve phosphorylation of multiple substrates that affect other cytoskeletal structures and proteins, such as LIM kinase, myosin light chain kinase, and Rho guanine nucleotide exchange factors (for a review, see Ref. 76). A previous study has illustrated the importance of the ERK (a MAPK) signaling pathway in regulating FA dynamics and cell motility (77). For instance, ERK is recruited to FAs in response to extracellular stimuli such as integrin engagement and activation of v-Src (78). FAK (and particularly Src-induced Tyr phosphorylation of FAK) is critical to the integration of migratory signals from integrins, possibly via Src, FAK, and the ERK or MAPK signaling pathway, to the calpain proteolytic system, resulting in FA turnover and cell migration. In brief, the modulation of FA dynamics utilized by these protein kinases apparently is reminiscent of the proposed β1-integrin/p-FAK Tyr^{397}/PI3K/PKB/PAK/ERK-mediated ES dynamics reported herein. For example, from 2 days post-treatment, the levels of PI3K p85α, PI3K p110α, PTEN, p-PKB Thr^{308}, p-PKB Ser^{473}, and PAK were significantly diminished, coinciding with the declining events of AJ disruption when virtually all elongating/elongated spermatids were depleted from the seminiferous epithelium in ~98% of the tubules examined, followed by the loss of round spermatids and most spermatocytes from the epithelium. These results further support the notion that these proteins are involved in AJ disassembly. This decrease in protein levels was also accompanied by a reduction of immunoreactive PI3K p85α, PKB, and p-PKB Ser^{473} levels detected in the seminiferous epithelium. It is of interest to note that immunoreactive PI3K p85α, PKB, and p-PKB Ser^{473} were not confined to the basal ES/BTB site, but apparently localized in the Sertoli cell cytoplasm after 4 days post-treatment. This finding suggests that PI3K/PKB may not be involved in TJ restructuring because the TJ was found to remain relatively intact after AF-2364 treatment (for a review, see Ref. 3).

We offer the following explanation for the surge of p-ERK1/2 during AF-2364-induced germ cell loss, which was further upregulated by wortmannin. It is known that the Ras/Raf/MEK/ERK and PI3K/PKB signaling pathways can cross-talk at the levels of Raf-1 and PKB, where PKB can phosphorylated Raf-1 at Ser^{259}, reducing Raf-1 activity. Such intriguing cross-talks between PKB and Raf depend on ligand types and concentrations (27). In this study, we have shown that inhibition of PI3K (and plausibly PKB indirectly) by wortmannin prior to AF-2364 treatment led to induction of p-ERK1/2 concomitant with a decline in p-PKB Thr^{308}. This observation suggests that the inhibitory effect is suppressed as a result of cross-talks between the two signaling pathways. As such, we can argue that induction of p-ERK1/2 by 8 h post-AF-2364 treatment and thereafter may be the result of declining PKB activity. It is noteworthy that insulin-like growth factor-1 at 10 ng/ml, which is optimal for mitogenesis and cell proliferation and motility, can activate the PI3K/Akt pathway, leading to Raf kinase inactivation and a transient ERK response; this in turn induces MMP-2 and its activation. At higher doses, however, activation of the ERK pathway appears to dominate without PI3K activation, and this leads to down-regulation of MMP-2 synthesis (79). It was recently shown that MMP-2 is induced and activated at the time of AF-2364-mediated ES disassembly; it is possible that such an induced MMP-2 production is regulated via the PI3K/PKB/ERK pathway. In summary, we have shown that the β1-integrin/p-FAK/PI3K/PKB/ERK signaling pathway is a putative regulatory channel that modulates the β1-integrin-mediated cell adhesion function between Sertoli cells and spermatids in the seminiferous epithelium during spermatogenesis, as depicted in Fig. 14.

AQ: GG

AQ: HH

AQ: II

AQ: JJ

AQ: KK

REFERENCES

1. Cheng, C. Y., and Mruk, D. D. (2002) *Physiol. Rev.* **82,** 825–874
2. Vogl, A. W., Pfeiffer, D. C., Mulholland, D., Kimel, G., and Guttman, J. (2000) *Arch. Histol. Cytol.* **63,** 1–15
3. Mruk, D. D., and Cheng, C. Y. (2004) *Endocr. Rev.* **25,** 747–806
4. Vogl, A. (1989) *Int. Rev. Cytol.* **119,** 1–56
5. Toyama, Y., Maekawa, M., and Yuasa, S. (2003) *Anat. Sci. Int.* **78,** 1–16
6. de Kretser, D. M., and Kerr, J. B. (1988) in *The Physiology of Reproduction* (Knobil, E., and Neill, J., eds) Vol. I, pp. 837–932, Raven Press, New York
7. Siu, M. K. Y., and Cheng, C. Y. (2004) *BioEssays* **26,** 978–992
8. Siu, M. K. Y., Mruk, D. D., Lee, W. M., and Cheng, C. Y. (2003) *Endocrinology* **144,** 2141–2163
9. Parsons, J. T. (2003) *J. Cell Sci.* **116,** 1409–1416
10. Chen, H. C., Appeddu, P. A., Isoda, H., and Guan, J. L. (1996) *J. Biol. Chem.* **271,** 26329–26334
11. Cantrell, D. A. (2001) *J. Cell Sci.* **114,** 1439–1445
12. Merlot, S., and Firtel, R. A. (2003) *J. Cell Sci.* **116,** 3471–3478
13. Foster, F. M., Traer, C. J., Abraham, S. M., and Fry, M. J. (2003) *J. Cell Sci.* **116,** 3037–3040
14. Brazil, D. P., Park, J., and Hemmings, B. A. (2002) *Cell* **111,** 293–303
15. Scheid, M. P., and Woodgett, J. R. (2003) *FEBS Lett.* **546,** 108–112
16. Marino, M., Acconcia, F., and Trentalance, A. (2003) *Mol. Biol. Cell* **14,** 2583–2591
17. Brazil, D. P., Yang, Z. Z., and Hemmings, B. A. (2004) *Trends Biochem. Sci.* **29,** 233–242
18. Munshi, H. G., Ghosh, S., Mukhopadhyay, S., Wu, Y. I., Sen, R., Green, K. J., and Stack, M. S. (2002) *J. Biol. Chem.* **277,** 38159–38167
19. Laprise, P., Chailler, P., Houde, M., Beaulieu, J. F., Boucher, M. J., and Rivard, N. (2002) *J. Biol. Chem.* **277,** 8226–8234
20. Guttman, J. A., Janmey, P., and Vogl, A. W. (2002) *J. Cell Sci.* **115,** 499–505
21. Meroni, S. B., Riera, M. F., Pellizzari, E. H., Galardo, M. N., and Cigorraga, S. B. (2004) *J. Endocrinol.* **180,** 257–265
22. Khan, S. A., Ndjountche, L., Pratchard, L., Spicer, L. J., and Davis, J. S. (2002) *Endocrinology* **143,** 2259–2267
23. Meroni, S. B., Riera, M. F., Pellizzari, E. H., and Cigorraga, S. B. (2002) *J. Endocrinol.* **174,** 195–204
24. Bokoch, G. M. (2003) *Annu. Rev. Biochem.* **72,** 743–781
25. Kumar, R., and Vadlamudi, R. K. (2002) *J. Cell. Physiol.* **193,** 133–144
26. Zhou, G. L., Zhuo, Y., King, C. C., Fryer, B. H., Bokoch, G. M., and Field, J. (2003) *Mol. Cell. Biol.* **23,** 8058–8069
27. Moelling, K., Schad, K., Bosse, M., Zimmermann, S., and Schweneker, M. (2002) *J. Biol. Chem.* **277,** 31099–31106

28. Chapin, R. E., Wine, R. N., Harris, M. W., Borchers, C. H., and Haseman, J. K. (2001) *J. Androl.* **22,** 1030–1052
29. Grima, J., Wong, C. C. S., Zhu, L. J., Zong, S. D., and Cheng, C. Y. (1998) *J. Biol. Chem.* **273,** 21040–21053
30. Mruk, D., and Cheng, C. Y. (1999) *J. Biol. Chem.* **274,** 27056–27068
31. Galdieri, M., Ziparo, E., Palombi, F., Russo, M. A., and Stefanini, M. (1981) *J. Androl.* **5,** 249–259
32. Mruk, D., Zhu, L. J., Silvestrini, B., Lee, W. M., and Cheng, C. Y. (1997) *J. Androl.* **18,** 612–622
33. Lui, W. Y., Mruk, D. D., Lee, W. M., and Cheng, C. Y. (2003) *Biol. Reprod.* **68,** 1087–1097
34. Lee, N. P. Y., Mruk, D., Lee, W. M., and Cheng, C. Y. (2003) *Biol. Reprod.* **68,** 489–508
35. Aravindan, G. R., Pineau, C., Bardin, C. W., and Cheng, C. Y. (1996) *J. Cell. Physiol.* **168,** 123–133
36. Strege, P. R., Holm, A. N., Rich, A., Miller, S. M., Ou, Y., Sarr, M. G., and Farrugia, G. (2003) *Am. J. Physiol.* **284,** C60–C66
37. Zwain, I. H., and Cheng, C. Y. (1994) *Mol. Cell. Endocrinol.* **104,** 213–227
38. Siu, M. K. Y., and Cheng, C. Y. (2004) *Biol. Reprod.* **70,** 945–964
39. Kustin, K., and Toppen, D. L. (1973) *J. Am. Chem. Soc.* **95,** 3563–3564
40. Przyborowski, L., Schwarzenbach, G., and Zimmermann, T. (1965) *Helv. Chim. Acta* **48,** 1556–1565
41. Crans, D. C. (1994) *Comments Inorg. Chem.* **16,** 1–33
42. Huyer, G., Liu, S., Kelly, J., Moffat, J., Payette, P., Kennedy, B., Tsaprailis, G., Gresser, M. J., and Ramachandran, C. (1997) *J. Biol. Chem.* **272,** 843–851
43. Crans, D. C., Bunch, R. L., and Theisen, L. A. (1989) *J. Am. Chem. Soc.* **111,** 7597–7607
44. Cheng, C. Y., Mather, J. P., Byer, A. L., and Bardin, C. W. (1986) *Endocrinology* **118,** 480–488
45. Mather, J. P., Zhuang, L. Z., Perez-Infante, V., and Phillips, D. M. (1982) *Ann. N. Y. Acad. Sci.* **383,** 44–55
46. Crepieux, P., Marion, S., Martinat, N., Fafeur, V., Le Vern, Y., Kerboeuf, D., Guillou, F., and Reiter, E. (2001) *Oncogene* **20,** 4696–4709
47. Crepieux, P., Martinat, N., Marion, S., Guillou, F., and Reiter, E. (2002) *Arch. Biochem. Biophys.* **399,** 245–250
48. Cheng, C. Y., Silvestrini, B., Grima, J., Mo, M. Y., Zhu, L. J., Johansson, E., Saso, L., Leone, M. G., Palmery, M., and Mruk, D. (2001) *Biol. Reprod.* **65,** 449–461
49. Grima, J., Silvestrini, B., and Cheng, C. Y. (2001) *Biol. Reprod.* **64,** 1500–1508
50. Lee, N. P. Y., and Cheng, C. Y. (2003) *Endocrinology* **144,** 3114–3129
51. Bradford, M. M. (1976) *Anal. Biochem.* **72,** 248–254
52. Laemmli, U. K. (1970) *Nature* **227,** 680–685
53. Wierzbicka-Patynowski, I., and Schwarzbauer, J. E. (2002) *J. Biol. Chem.* **277,** 19703–19708
54. Cheng, C. Y., Mathur, P. P., and Grima, J. (1988) *Biochemistry* **27,** 4079–4088
55. Siu, M. K. Y., and Cheng, C. Y. (2004) *Biol. Reprod.* **71,** 375–391
56. Cunningham, C. C., Vegners, R., Bucki, R., Funaki, M., Korde, N., Hartwig, J. H., Stossel, T. P., and Janmey, P. A. (2001) *J. Biol. Chem.* **276,** 43390–43399
57. Payrastre, B., Missy, K., Giuriato, S., Bodin, S., Plantavid, M., and Gratacap, M. (2001) *Cell. Signal.* **13,** 377–387
58. Raucher, D., Stauffer, T., Chen, W., Shen, K., Guo, S., York, J. D., Sheetz, M. P., and Meyer, T. (2000) *Cell* **100,** 221–228
59. Sander, E. E., van Delft, S., ten Klooster, J. P., Reid, T., van der Kammen, R. A., Michiels, F., and Collard, J. G. (1998) *J. Cell Biol.* **143,** 1385–1398
60. Braga, V. M., Machesky, L. M., Hall, A., and Hotchin, N. A. (1997) *J. Cell Biol.* 1421–1431
61. Braga, V. M., Del Maschio, A., Machesky, L., and Dejana, E. (1999) *Mol. Biol. Cell* **10,** 9–22
62. Somasiri, A., Wu, C., Ellchuk, T., Turley, S., and Roskelley, C. D. (2000) *Differentiation* **66,** 116–125
63. King, C. C., Gardiner, E. M. M., Zenke, F. T., Bohl, B. P., Newton, A. C., Hemmings, B. A., and Bokoch, G. M. (2000) *J. Biol. Chem.* **275,** 41201–41209
64. Lee, N. P. Y., and Cheng, C. Y. (2005) *J. Cell. Physiol.* **202,** 344–360
65. Renkema, G. H., Pulkkinen, K., and Saksela, K. (2002) *Mol. Cell. Biol.* **22,** 6719–6725
66. Pedram, A., Razandi, M., and Levin, E. R. (2002) *J. Biol. Chem.* **277,** 44385–44398
67. Zhang, M., Waelde, C. A., Xiang, X., Rana, A., and Luo, Z. (2001) *J. Biol. Chem.* **276,** 25157–25165
68. Daub, H., Gevaert, K., Vandekerckhove, J., Sobel, A., and Hall, A. (2001) *J. Biol. Chem.* **276,** 1677–1680
69. Amlani, S., and Vogl, A. W. (1988) *Anat. Rec.* **220,** 143–160
70. Ohtakara, K., Inada, H., Goto, H., Taki, W., Manser, E., Lim, L., Izawa, I., and Inagaki, M. (2000) *Biochem. Biophys. Res. Commun.* **272,** 712–716
71. Goto, H., Tanabe, K., Manser, E., Lim, L., Yasui, Y., and Inagaki, M. (2002) *Genes Cells* **7,** 91–97
72. Carragher, N. O., and Frame, M. C. (2004) *Trends Cell Biol.* **14,** 241–249
73. Cenni, V., Sirri, A., Riccio, M., Lattanzi, G., Santi, S., de Pol, A., Maraldi, N. M., and Marmiroli, S. (2003) *CMLS Cell. Mol. Life Sci.* **60,** 2710–2720
74. Sells, M. A., Pfaff, A., and Chernoff, J. (2000) *J. Cell Biol.* **151,** 1449–1458
75. Sells, M. A., Knaus, U. G., Bagrodia, S., Ambrose, D. M., Bokoch, G. M., and Chernoff, J. (1997) *Curr. Biol.* **7,** 202–210
76. Hofmann, C., Shepelev, M., and Chernoff, J. (2004) *J. Cell Sci.* **117,** 4343–4354
77. Webb, D. J., Donais, K., Whitmore, L. A., Thomas, S. M., Turner, C. E., Parsons, J. T., and Horwitz, A. F. (2004) *Nat. Cell Biol.* **6,** 154–161
78. Fincham, V. J., James, M., Frame, M. C., and Winder, S. J. (2000) *EMBO J.* **19,** 2911–2923
79. Zhang, D., Bar-Eli, M., Meloche, S., and Brodt, P. (2004) *J. Biol. Chem.* **279,** 19683–19690

AQ: LL

AUTHOR QUERIES

AUTHOR PLEASE ANSWER ALL QUERIES 1

A—Please provide the postal code for Hong Kong.

B—"ES likely utilizes" as meant?

C—If your Abstract runs over into the right-hand column, please cut text to fit into the left-hand column only.

D—Changes have been made throughout to standard English. **Please read your page proofs carefully to check that they reflect your meaning.**

E—"PI3K" is the abbreviation preferred by the Journal.

F—"polyphosphoinositides" as meant here and in Footnote 1? If not, please explain the extra "P" in PPI."

G—"phosphoinositide-dependent" as meant here and in Footnote 1?

H—"deleted" as meant?

I—"Wilmington" as meant?

J—Please confirm that "v/v" is correct here.

K—"cheating" changed to "chelating" here and once below.

L—Please check that the sentence beginning "One of the apparent targets" is worded clearly.

M—Ref. 3 as meant?

N—If "anti-β1-integrin IgG" should be "anti-β1-integrin antibody," please correct page proofs here and below.

O—"fluorescein isothiocyanate-labeled" as meant?

P—Please check sentence beginning "A tubule from rats. . . " for clarity and rewrite if necessary.

Q—"see *white arrowhead* in Fig. 1*G*" as meant?

R—If "induced" should be "increased," please correct page proofs.

S—"resulted in an increase in" as meant?

T—Please confirm/correct changes made to sentence beginning "For instance. . . "

AUTHOR QUERIES

AUTHOR PLEASE ANSWER ALL QUERIES 2

U—"an ~6-fold increase" as meant?

V—"Moderate staining" as meant?

W—Please correct "XII–III."

X—Please correct "XII–V."

Y—"PI3K" as meant per Fig. 8*A*?

Z—"pull down" as meant here and below?

AA—"inhibitor" instead of "kinase" as meant?

BB—"had no effect on the delay" as meant?

CC—"including" as meant?

DD—"MTM proteins" as meant? If not, please provide a suitable plural noun.

EE—Quotation marks deleted after first in text use per Journal style.

FF—If "functionally at the ES site" should be "at the functional ES site," please correct page proofs.

GG—Please confirm/correct changes made to sentence beginning "This observation suggests. . . "

HH—Please cite reference for "It was recently shown."

II—Paragraph continued to avoid a one-sentence paragraph.

JJ—Please confirm journal title in Ref. 5.

KK—Please cite Ref. 15 in text, or we will replace with "Deleted in proof." **PLEASE DO NOT** renumber references for any reason.

LL—Please confirm journal title in Ref. 41.

MM—Please provide postal code for Hong Kong.

NN—Please define "*Ac*" and "*N*" in the legend to Fig. 1.

OO—Please check the colors on the computer screen against what is mentioned in the legend and amend the legend as necessary. Please review the reproduction quality of all color figures and

AUTHOR QUERIES

AUTHOR PLEASE ANSWER ALL QUERIES

note clearly any concerns. Are the color figures acceptable for publication?

PP—"kg of body weight" as meant?

QQ—"*I–L*" as meant?

RR—Quotation marks deleted after first use per Journal style.

SS—Please define "*PRII*" and "*PRI*" in the legend to Fig. 14.